UNIVERSITY OF CALIFORNIA,
IRVINE

Foraging behaviors mediated by the lateral line in zebrafish (*Danio rerio*)

DISSERTATION

submitted in partial satisfaction of the requirements
for the degree of

DOCTOR OF PHILOSOPHY

in Biological Sciences,

by

Andres Carrillo

Dissertation Committee:
Professor Matthew J. McHenry, Chair
Senior Lecturer SOE Catherine Loudon
Associate Professor Donovan P. German

2018

DEDICATION

To

Nico and JoJo Bravo

TABLE OF CONTENTS

	Page
LIST OF FIGURES	iv
LIST OF TABLES	v
ACKNOWLEDGMENTS	vi
CURRICULUM VITAE	vii
ABSTRACT OF THE DISSERTATION	viii
INTRODUCTION	1
CHAPTER 1: Zebrafish learn to forage in the dark	7
Introduction	7
Material and Methods	9
Results	16
Discussion	25
CHAPTER 2: Canal neuromasts enhance foraging in zebrafish	29
Introduction	29
Material and Methods	32
Results	39
Discussion	46
CHAPTER 3: Forces detected by the receptors of the lateral line system of zebrafish	50
Introduction	50
Material and Methods	52
Results	58
Discussion	69
REFERENCES	72

LIST OF FIGURES

		Page
Figure 1.1	Effects of the lateral line system in *Danio rerio* on foraging with age	20
Figure 1.2	Effects of the cranial lateral line on foraging	21
Figure 1.3	Total number of neuromasts with age	22
Figure 1.4	Morphology of cranial neuromasts with age	23
Figure 1.5	Effects of learning on foraging performance in the dark	24
Figure 2.1	Experimental setup for behavioral experiments	38
Figure 2.2	The behavioral frequency response to a vibrating rod	42
Figure 2.3	Experimental manipulation of the lateral line system in adult zebrafish	43
Figure 2.4	The probability of exhibiting vergence for treatment and age groups	44
Figure 2.5	Response distance to the vibrating rod stimulus	45
Figure 3.1	Flow visualization of stimulus created by oscillating rod	64
Figure 3.2	The behavioral frequency response and sensitivity to a vibrating rod	65
Figure 3.3	Biophysical models of cranial neuromasts, based on morphometric measurements	66
Figure 3.4	Response distance to the vibrating rod stimulus (From Chapter 2).	67
Figure 3.5	Modeled responses of SNs and CNs in behavioral experiments	68

LIST OF TABLES

		Page
Table 3.1	Spatial decay in flow velocity	62
Table 3.2	Morphometrics of the lateral line	63

ACKNOWLEDGMENTS

I would like to express the deepest appreciation to my committee chair, Professor Matthew James McHenry, who has been an amazing advisor. He has provided me training and guidance, and is someone I happily call my advisor, mentor, and role model. He helped me get through the tough times while I was in grad school, in which without the support he provided, would not have been possible.

I would like to thank my committee members, Drs. Donovan German and Catherine Loudon, whose support and discussions helped me develop and improve the quality of my dissertation. They both have served as great instructor and research role-models, which I hope to pass on. A special shout out to Dr. German who helped me get though one of the toughest times in my life.

In addition, I would like to thank all members in the 210 group, whom helped improved professional development sessions, which supported my research goals and career ambitions. I have made many great friends in this group, whose friendship and support I will cherish forever. An especial thanks to the four As (my labmates) for their help and support over the years.

I would like to thank my family, especially Nico, who continually helped me recognize the value of linking science to community. Thank you for giving me purpose in life. I would like to thank my dear friends: Laura Elsberry, Justin Grimes, and Arthur Wu who supported me like family though this endeavor.

I thank many undergraduate students, Peter Abdelmesseh, Cody Angulu, David Garcia, Christopher Glaubensklee, Dan Van Le, Johnny Nguyen for their help with project development, data collection, and data analysis, for the projects presented here and additional side projects.

Lastly, I thank the Company of Biologist for permission to include copyrighted materials in this dissertation, which was originally published in the Journal of Experimental Biology (2016). Financial support was provided by the Graduate Division and the Department of Ecology and Evolutionary Biology at the University of California, Irvine, The California State University Pre-Doctoral Incentive Program, the United States Department of Agriculture: Watershed Doctoral Management Program, the National Science Foundation Grant (IOS-1354842 and IOS-0952344) and an Office of Naval Research (N00014-15-1-2249).

CURRICULUM VITAE

Andres Carrillo

EDUCATION

2018 Ph.D. in Biological Sciences, concentration: Ecology and Evolutionary Biology, University of California, Irvine, CA
Advisor: Matthew J. McHenry

2012 M.S. in Biology, California State University, Fullerton, CA.
Advisor: Kathryn A. Dickson

2008 B.S. in Biological Sciences, California State University, Fullerton, CA.
Concentration: Marine Biology

APPOINTMENTS

2018 Research Curator, Aquatic Nursery
Cabrillo Marine Aquarium, Los Angeles, CA

2002-2017 Outreach research coordinator, Aquatic Nursery
Cabrillo Marine Aquarium, Los Angeles, CA

2012-2018 Teaching Assistant, School of Biological Sciences,
University of California, Irvine

PUBLICATIONS

Aryafar, H.A., Carrillo, A., Berquist, R., Frank, L.R., Forsgren, K.L., and K.A. Dickson (IN REVIEW) Description of a Male Urogenital Papilla in the California Grunion, *Leuresthes tenuis,* a Beach-spawning Marine Silverside Fish. *Bull. South. Calif. Acad. Sci.*

Santos, A.J., Frederick, A.R., Higgins, B.A., Carrillo, A., Carter, A.L., Dickson, K.A, German, D.P., and M.H. Horn (2018) The beach-spawning California grunion *Leuresthes tenuis* eats and digests conspecific eggs. *J. Fish Biol.* 93, 282-289

Carrillo, A. and M.J. McHenry (2016). Zebrafish learn to forage in the dark. *J. Exp. Biol.* 219, 582-589

ABSTRACT OF THE DISSERTATION

Foraging behaviors mediated by the lateral-line system in zebrafish (*Danio rerio*)

By

Andres Carrillo

Doctor of Philosophy in Biological Sciences,

With a concentration in Ecology and Evolutionary Biology

University of California, Irvine, 2018

Professor Matthew James McHenry, Chair

Successful foraging is crucial to the energetic demands of fishes, but the role of lateral-line system during feeding remains unclear. In this dissertation I investigated how the lateral line mediates foraging throughout ontogeny of zebrafish. The results demonstrate the fish need the lateral-line system to successfully feed in the dark, and the types of lateral-line receptors play an important role during foraging.

My first chapter developed a series of lateral-line manipulations to test how flow receptors influences foraging success. I also examined the morphology of the receptors to determine if morphological changes in the receptors during early growth may improve flow sensitivity. The results suggest that the lateral line is not important when foraging in light, but in the dark, that lateral line is necessary. In addition, the receptors do not increase in size or numbers during early growth to explain improved sensitivity during growth, however, experiences to flows throughout development suggests that fish learn to forage on prey in 15-day old larvae.

In my second chapter, I investigated how zebrafish respond to various frequencies of oscillating flow in the dark created by an artificial stimulus resembling prey. I compared the bite attempts of fish with different lateral line profiles, presence or absence of receptors, to determine if growth enhances the ability of fish to detect flows in the dark. This improvement was greater at high oscillating-frequencies (above 50 Hz), compared to those below 50 Hz, suggesting that canal neuromasts, which develop in adults, improve foraging in the dark.

I modeled the sensitivity of the lateral-line receptors exposed to flows generated by the artificial stimulus in chapter three. A biophysical model predicting neuromast sensitivity was evaluated with the parameters of flows and zebrafish used in chapter 2. The flows generated by stimuli were measured using a novel digital partial image-velocimetry technique to determine which flows fish responded to in the dark. The biophysical model and flows suggest that fish respond best with the canal neuromasts, and the lateral line receptors exist as a network allowing fish to detect flows at great distances.

INTRODUCTION

Fish must be able to successfully forage to obtain energy to ensure energetic demands of growth, thus, affecting survival. The foraging behaviors and kinematics of feeding have been classically studied, with interests towards the sensor-motor control mechanisms that mediate feeding. However, the role of the lateral line, the mechanosensory system of fish during feeding remains unclear, especially during early development. The purpose of this dissertation was to investigate how the lateral-line system influences foraging throughout ontogeny and development to clarify how fish respond to prey using their lateral line.

Foraging behavior in fish can be described as a four-step process: (1) food detection, (2) food localization, (3) food capture, and (4) ingestion (Atema, 1971). During food detection, fish sense a potential food item typically using visual and chemical cues (Muto and Kawakami, 2013; Li et al., 2005). This is immediately followed by step 2, food localization, in which fishes deploy swimming maneuvers to orient their heading towards the food item (Budick and O'Malley, 2000; O'Malley et al., 2004), with the goal of reducing the distance between the fish and its food to favor a bite attempt (McElligott and O'Malley, 2005). Food capture (step 3) occurs when a fish can successfully coordinate its position and heading to the food to successfully capture the food during a bite. This step is challenging because fish must coordinate their movements to that of the food item, especially when hunting mobile prey. For successful ingestion (step 4) the food item must be of appropriate size and positioned in the mouth that is ideal for swallowing.

Food detection by fishes

Early detection of food can be achieved with one or multiple sensory modalities by fish (Wright et al., 2005; Westphal and O'Malley, 2013). Vision has been shown to be the primary sensory system used by fish to detect food and indicating that species studied are primarily visual

predators (Gahtan and O'Malley, 2003; Gahtan et al., 2005). Fishes may utilize other sensory modalities for food detection, such as olfactory and auditory sensing (Dempsey, 1978; Margullies, 1983; Wright et al., 2005). In addition, The lateral line system is the mechanosensory system is used by fish to detect flows, and is also known to detect foods items, especially in prey that create perturbations in the water as they swim (McElligott and O'Malley, 2005; Westphal). Visual detection of food typically occurs at distances that are usually beyond the abilities of the mechanosensory capabilities of fish, but in the absence of vision, such as in the dark or low-visibility habitats fish may rely on this system (McElligott and O'Malley, 2005; Westphal et al., 2013).

While searching for food, fish swim in a sweeping pattern in attempts to visually detect food (Muki et al., 2013; Patterson et al., 2013; Fig. 3). While swimming in a sweeping fashion, fishes increase the chance of encountering foods by exploring more area, which is important for fishes that feed on immobile foods (Budick and O'Malley, 2000). Alternatively, feeding on mobile prey provides additional visual stimuli that alert fish to foods. For example, prey detection has been investigated in free-swimming zebrafish (*Danio rerio*) larvae exposed to live prey (*Paramecium* sp.), which deploy a series of eye movements and swimming maneuvers upon detecting prey (Gahtan et al., 2005, Fig. 4). Eye tracking are independent eye movements that track prey as the fish stereotypically follows the food with turns to orient food towards the mouth. Eye convergence occurs when a fish medially rotates its eyes to increase binocular vision, which increases depth of view to the prey improving localization. Both eye movements are used upon detection and assists with localization of foods in fish.

Eye movements have been documented in many species following alert to prey. Herring (*Clupea* sp.) larvae feeding freely on live prey use these eye movements when they detect a

potential food source (Dempsey, 1978). In a study by Patterson et al., (2013), tethered zebrafish larvae presented with a moving dot (of similar size and speed of typical prey) projected on a screen elicited eye-tracking movements to follow the position of the dot. Vision clearly serves as the primary sensory modality used by fish to detect foods, however, environmental conditions can hinder the use of vision, such as the occurrences of cloudy or turbid water, in which, light becomes limited. Studies suggest that fish rely on additional sensory modalities to detect foods, such as olfactory cues (Budick and O'Malley, 2000; Gahtan et al., 2005, Dempsey, 1978). Auditory and mechanosensory signals have also been shown to initiate localization behaviors in fishes. Some fish even display foraging behaviors in response to auditory recordings of actively feeding conspecifics (Wright et al., 2005).

In a study on zebrafish larvae, the lateral line systems, the mechanosensory organ, is used to detect flows of prey leading to successful capture, suggesting that fish larvae can detect prey in the absence of light (Westphal et al., 2013, Carrillo and McHenry, 2016). Larvae deprived of the lateral line system in the dark feed poorly, when compared to those with a functional lateral line. This indicates that the mechanosensory systems in fish can be used to detect and localize food in the absence of vision, but has a limited distance as flow signals decay, which is estimated to be half of the body length of a fish (Westphal et al., 2013).

Search and localization of food

Upon detecting potential foods, fishes deploy stereotypical foraging behaviors, which include eye-tracking, subtle maneuvered turns (called: j-turns), and pursuit swimming bursts as they attempt to localize a potential food source. The search typically begins with eye tracking that allow larvae to target and pursuit a potential food (Gahtan and O'Malley, 2003; Gahtan et al., 2005). This is followed by the orientation phase, in which larvae complete swimming maneuvers

to create small movements that position a fish into an ideal position to capture the food item. These specialized swimming turns are used to move the axis of the body to an orientation that directs the head towards the food to position of the fish's head at a distance ideal for a bite (Patterson et al., 2013; Westphal and O'Malley, 2013)

Foraging-swimming behaviors are the serve as visual activities indicative of search behaviors when fish forage. Once fish detect food, they initiate foraging-swimming behaviors, however, it can be difficult to differentiate foraging to volitional swimming in most researched species, thus, search-swimming behavior may not be best to describe detecting in fishes in details compared to other behaviors elicited when localizing food, such as eye tracking.

The onset of pursuit swimming behaviors in fishes are mainly observed as the fish prepares its bite attempts. Eye-tracking and convergence may be included during the pursuit, as they allow a fish to determine the position of the food between swimming bouts (Budick and O'Malley, 2000; Bianco et al., 2011, McElligott and O'Malley, 2005). As previously mentioned, vision is not always available to larvae when feeding and some fish feed in the dark. The lateral-line system, mechnosensory organ, of fish detects water flows generated by swimming prey. This is achieved through deflections of the lateral line receptors, called neuromasts. Adult fishes use the mechansensory cues to localize and capture prey, but as larvae the have a fewer, smaller, and less developed neuromasts that compose the lateral line (Webb and Shirley, 2003).

Until recently, it was unclear if larvae could use mechanosory cues to localize prey. Westphal et al. (2013) described foraging behaviors, resembling detection and search activities, mediated by the lateral line in larval and juvenile zebrafish. Interestingly the absence of the lateral line in the presence of light did not impede feeding as it did in the dark. Thus, for species that feed in the light, vision remains the primary modality used to localize and capture prey, but

it is possible for those fish to use the mechanosensory organs to feed. It remains unclear how crucial the lateral line system is for feeding, as it could be used for multimodal sensing, coupled with other senses to provide fish with various information in the pursuit of food.

Flow detection with the lateral line

Most teleost fishes possess the lateral-line system, which facilitates the sense to water flow with mechanoreceptors on skin. This receptor includes an elongated structure that extends into the water, and it is deflected by the surrounding hydrodynamic forces (Dijkgraaf, 1963). The deflection of this structure is then detected by the nervous signal by mechanosensory cells anchored within the skin attached to the receptors. In fishes (Dijkgraaf, 1963; Coombs and Montgomery, 1999) and amphibians (Scharrer, 1932), these receptors are known as superficial neuromasts (SNs), and they include a cluster of hair cells that are deflected by flows acting on the cupula, the protruding structure that is deflected, that is extended into the environment. As larvae, zebrafish only possess SNs in their lateral line (Webb and Shirley, 2003; Carrillo and McHenry, 2016), which provides sufficient information to detect food (Patterson et al., 2013; Westphal and O'Malley, 2013) and predators (Stewart et al., 2014; Nair et al., 2017).

The lateral line of teleost fishes is unique among animal taxa because it also includes a second type of receptor, the canal neuromast (CN) which forms as fish grow into the juvenile and adult stage (Webb and Shirley, 2003). A CN resides within a canal beneath the body's surface, which are generally opened to the surface via pores that detect differences in pressure between pores. Due to the distinct sensitivity of SNs and CNs, the fish lateral line is described as possessing two submodalities of flow sensing (Coombs and Montgomery, 1999). It remains unclear how a fish benefits from having CNs in addition to

SNs. Therefore, the aim of this work was to determine how SNs and CNs play a role during foraging in zebrafish as they grow, which consequently results in different morphological profiles of neuromasts as they grow from larvae to juveniles.

The current dissertation

In this article, I have developed three studies in which the lateral-line system was investigated how it affects foraging behavior. Using various experimental manipulations, I examined how the presence SNs and CNs influence the foraging ability in zebrafish. These behaviors were examined on flows generated by live prey and a controlled stimulus to accurately describe the types of flows fish respond when foraging. With the use of models, the sensitivities of the lateral-line system was modeled using the flow profiles experienced by fish in this study. All together these studied demonstrate the importance of the lateral line and its development to foraging abilities of zebrafish.

CHAPTER 1: ZEBRAFISH LEARN TO FORAGE IN THE DARK

Introduction

The ability to sense prey during foraging is critical to the early growth and survival of fishes. Although vision is essential, larval zebrafish (*Danio rerio*) can forage on zooplankton in the dark by sensing water flow with the lateral-line system (LLS) (Westphal and O'Malley, 2013). The LLS serves this function with a series of mechanoreceptors in the skin called superficial neuromasts (Dijkgraaf, 1963). These neuromasts presumably allow a fish to detect the perturbations created by the propulsion of prey. However, it is not clear how this is achieved, and it is therefore unknown what properties of the LLS matter to foraging performance. The present study examined how zebrafish acquire the ability to forage in the dark over their first month of age. A number of studies have examined the foraging behavior of larval zebrafish. Larvae begin foraging after the swim bladder inflates, which occurs 1 day after hatching and at 5 days post fertilization (dpf). Foraging is characterized by spontaneous intermittent swimming that is interrupted by targeted movement toward prey upon detection (Fuiman and Webb, 1988; Budick and O'Malley, 2000). This targeted swimming includes a series of pectoral fin and tail motions that serve to align the rostrum with the prey (McElligott and O'Malley, 2005; Patterson et al., 2013). Once in a close position (<0.5 mm), the larva attempts to capture the prey with a suction-feeding strike (Patterson et al., 2013).

Although foraging proceeds similarly in the dark, vision greatly enhances a larva's ability to detect prey. Under illumination, larvae respond to zooplankton at a greater distance (<3 mm) compared to the dark (<1 mm) (Gahtan et al., 2005; Bianco et al., 2011; Patterson et al., 2013). Larvae strike at prey in the dark with a relatively low frequency and each strike is less successful than when they can see (Westphal and O'Malley, 2013). Whether mediated by vision or other sensory systems, the strike rate and capture probability increase with age, perhaps through a combination of changes in sensory perception, neuromuscular control, jaw development, and hydrodynamics (Easter and Nicola, 1996; Hernandez, 2000; Hernandez et al., 2005; McHenry and Lauder, 2006; Danos and Lauder, 2007; Green and Hale, 2012; Staab and Hernández, 2010; China and Holzman, 2014).

It is not clear whether improvements in foraging with age are related to the development of the LLS. Upon hatching, the LLS includes approximately 24 superficial neuromasts on each side of the body, with nearly half positioned on the head at high density. Superficial neuromasts on the trunk may increase in number by a factor of two or three in the first month of age (Metcalfe et al., 1985; Ghysen and Dambly-Chaudièr e, 2007; Nuñez et al., 2009). After this period, many of the cranial superficial neuromasts transform into canal neuromasts by enlarging and becoming enclosed in bony canals with pores that open at the body's surface (Webb and Shirey, 2003). These morphological changes alter the frequency response of the neuromasts such that they become sensitive to pressure gradients in the flow field (van Netten, 2006). These changes are likely to be important to foraging because larval fish appear to be responsive to prey motion around the head (Bianco et al., 2011; Patterson et al., 2013). The present study included a morphological analysis of the superficial neuromasts during larval growth to test whether changes in morphology might account for the improvement of foraging in the dark with age.

Zebrafish larvae may alternatively enhance their foraging by learning to identify the flow that prey generate. This would appear to be possible because zebrafish are capable of associative learning. For example, adults can be trained to exhibit feeding behavior in response to a conditioned olfactory stimulus under classical conditioning (Braubach et al., 2009). From an early age, zebrafish are also responsive to operant conditioning. For example, larvae can be trained to orient their swimming to visual cues by negative reinforcement with an electric shock, and they improve in this task with age to the extent that larvae perform almost flawlessly by 4 weeks of age (Valente et al., 2012). The present study tested whether improvement in foraging in the dark is a consequence of associative learning by measuring the foraging of fish that were experimentally restricted from exposure to the flow of prey.

Materials and Methods

I tested the role of the LLS in the foraging of zebrafish by comparing rates of prey strikes and captures between fish with a compromised lateral line system and control fish. These experiments were performed on fish that varied in age, from hatchling larvae to 1-month-old juveniles. I tested whether the role of flow sensing differs when aided by vision by performing these experiments both in the dark and under illumination visible to the fish. Upon confirming reports finding that foraging improves with age and that the LLS is necessary for improved foraging, I tested hypotheses about this improvement. I addressed whether foraging is mediated primarily by the cranial lateral line by compromising only that region. Morphometrics of superficial neuromasts tested whether flow sensing is augmented by heightened sensitivity to flow (McHenry et al., 2008; Van Trump and McHenry, 2008). Finally, I raised fish that were naïve to the flow of *Artemia* to test the effects of associative learning.

Animal husbandry

Adult zebrafish, *Danio rerio* (Hamilton, 1922), were bred from wild-type (AB line) colonies that were housed in a flow-through aquarium system (Aquatic Habitats, Apopka, FL, USA) and maintained at 27°C on a 14 h:10 h light:dark cycle. Fertilized eggs from random mating pairs were cultured using standard rearing techniques (Westerfield, 1993). Larvae were raised in 3-liter tanks and were fed pellets (Larval AP100, Ziegler Bros, Gardens, PA, USA) from ages 5 to 30 dpf. This diet was enriched daily by feeding larvae live rotifers, *Brachionus plicatillis*, from 5 to 10 dpf, and *Artemia franciscana* nauplii from 7 to 30 dpf. Under these conditions, our fish attained a body length of 9.02±0.13 mm (N=15) by the age of 30 dpf. This period spans the duration of larval growth, with the oldest fish perhaps initiating juvenile development (Schilling, 2002; Brand et al., 2002). I therefore will refer to the younger (<25 dpf) fish in the present study as 'larvae' and the older fish (25 and 30 dpf) as 'juveniles'. With the exception of the experimental groups used to test the effects of learning (described below), all fish were fed under illumination throughout the rearing period and were therefore provided the opportunity to associate the appearance of prey with their water flow. All rearing and experimental protocols were conducted with the approval of the Institutional Animal Care and Use Committee at the University of California, Irvine.

Foraging experiments

Foraging experiments with *Artemia nauplii* were video-recorded. A single fish and approximately 15 nauplii (1-day post-hatch) were placed in a cylindrical arena (watch glass, 40 mm diameter×3 mm max. depth) with a glass cover to reduce distortions at the surface. A camera (Marlin, Allied Vision Technologies, Stadtroda, Germany) was positioned above the arena to

record feeding experiments (760×480 pixels, 5×5 cm field of view at 14.7 frames s^{-1}). Infrared panels (850 nm) were positioned below the arena with a diffuser (Parafilm sheet, 'M' Film, Pechiney Plastic Packaging, Chicago, IL, USA) to generate transmitted illumination for high-contrast videos with light not visible to the larvae. A 25 W fluorescent bulb was directed away from the arena to provide visible light for experiments under illuminated conditions. Prior to the experiments, all fish were fasted for 24 h to ensure motivation to feed during experiments.

I video-recorded foraging over a 10-min period. When reviewing these videos, I noted the number of instances that the fish visibly struck at prey and the number of those strikes that succeeded in capturing prey. These measurements provided the basis for three metrics of foraging performance: (1) the strike rate (the number of strikes per minute) served as an indication of the foraging activity of a larva; (2) the capture rate (the number of prey successfully acquired per minute) offered a general metric of feeding success; and (3) the capture probability (the ratio of capture rate to strike rate) indicated the overall effectiveness of feeding strikes.

Experimental manipulation of the LLS

I tested the role of the LLS by experimentally compromising its ability to sense flow. This was achieved by placing fish in a 250 μmol l^{-1} solution of neomycin sulfate (Fisher BioReagents, Fair Lawn, NJ, USA) for 45 min prior to experiments. This treatment kills most hair cells in the neuromasts (Harris et al., 2003; Van Trump et al., 2010), but leaves the hair cells of the inner ear intact and thereby has no adverse effect on sensing sound, body orientation, or acceleration. Experiments were performed within 2 h of the treatment because of the rapid ability of these hair cells to regenerate (McHenry et al., 2009). Fish were only used if they exhibited routine swimming behavior and motivation to feed. These experiments were performed on zebrafish of

varying age (7, 10, 12, 13, 15, 20, 25, and 30 dpf) to consider the effects of age on foraging performance.

Experiments were conducted to test the role of the LLS with and without the aid of vision. Untreated (i.e. with LLS) and treated (i.e. without the LLS) fish were filmed in either the light or dark at all ages (N=480). The mean values and 95% confidence intervals of our measurements of capture rate, strike rate, and capture probability were compared between untreated and treated groups. All statistical procedures for these experiments, and all others described in this study, were completed with custom scripts in MATLAB (v.2013a), available upon request from the corresponding author.

I tested the degree to which feeding depends on flow sensing by cranial neuromasts. These experiments were prompted by preliminary recordings and observations in the literature (e.g. Westphal and O'Malley, 2013), which showed that fish tended to pursue *Artemia* near the head when foraging in darkness. I developed a method to compromise flow sensing in the head while leaving the rest of the body unaltered. This was achieved by embedding the body of an anesthetized (0.0017 g l^{-1} of buffered MS-222; Finquel, Argent Chemical Laboratories, Redmond, WA, USA) juvenile (25 dpf) in a block of 5% agarose (low-melting point; Fisher Scientific, Fair Lawn, NJ, USA; heated to 60°C and cooled to 35°C). Once set, the agarose surrounding the head was removed with a scalpel to expose the head while leaving the body embedded. This served to protect the body, but not the head, from exposure to the neomycin solution for 45 min. The Petri dish was filled with a solution of neomycin sulfate (250 μmol l^{-1}) to act on only the exposed cranial neuromasts. After a recovery period (10 min), foraging experiments were performed in the manner described above. I was unable to devise a comparable

approach to compromise just the trunk lateral line because embedding the head in agarose prohibited the operculum from circulating the gills. I additionally performed a sham treatment where fish were anesthetized and embedded in agarose, but the head was exposed to water lacking neomycin.

Comparisons of capture and strike rates between treatment, control, and sham groups were performed by one-way ANOVA. This test was appropriate because the measurements were normally distributed (Kolmogorov–Smirnov, $P>0.05$) and showed homogeneity of variance (Levene's test, $P>0.05$). A Tukey's HSD test was performed to determine significant differences between groups. Capture probabilities were compared between groups with a Kruskal–Wallis test, because these data did not meet the assumption of a normal distribution. Pairwise comparisons, using a Nemenyi test (using a Tukey distribution), determined significant differences between groups.

Lateral-line morphometrics

I tested whether the improvements in foraging with age were reflected in changes in lateral-line morphology. Our morphometric analysis focused on the cranial LLS because our preliminary results suggested a major role for this region in foraging. I measured the number of neuromasts and, for each neuromast, the number of hair cells and the diameter (at the base) and height of the cupula. The cupula is an extracellular component of a superficial neuromast that extends from the surface of the body. The dimensions of the cupula and number of hair cells are the major structural features that determine the sensitivity of a superficial neuromast (McHenry et al., 2008; Van Trump and McHenry, 2008; van Netten and McHenry, 2013). These measurements were performed for the supraorbital (SO1–SO4), infraorbital (IO1–IO3), and mandibular (MN1–

MN3) neuromasts in fish of varying age (15, 25, and 30 dpf). Hair cells were visualized in anesthetized larvae embedded in agarose (0.5%) with a live fluorescent stain [0.02% DASPEI, 2-(4-(dumethylamino) styryl)-N-ethylpyridinium iodide; Invitrogen, Eugene, OR, USA], using a stereomicroscope (Zeiss Discovery V.20, Carl Zeiss, Thornwood, NY, USA) with a GPF filter set (450–490 nm) and fluorescence illuminator (120 W Mercury Vapor Short Arc, X-Cite series 120q, Lumen Dynamics, Mississauga, ON, CA).

Cupulae were visualized in a separate group of anesthetized fish that were perfused with polystyrene microspheres (0.1 μm diameter, Polysciences, Warrington, PA, USA). The microspheres adhered to the surface and provided sufficient contrast to see the peripheral shape of the cupula (Van Trump and McHenry, 2008) under Nomarski optics using a compound microscope (Zeiss Axioskop 2 FS plus, Carl Zeiss). The cupula diameter was measured from photographs (AxioCam HRc, Carl Zeiss) taken with the microscope focused on the base of the cupula. The diameter is a sufficient descriptor of the base dimensions because our preliminary observations found the base to be circular in shape. The cupula height was measured by noting the z-position of the microscope as I focused between the base and distal edge of the cupula. I performed a one-way ANOVA with post hoc comparisons (Tukey's HSD test) for all of these measurements to test the effect of age. These measurements met the assumptions of a normal distribution (Kolmogorov–Smirnov, $P>0.05$) and homogeneity of variance (Levene's test, $P>0.05$).

Learning experiments

I conducted experiments that tested whether zebrafish learn to use their LLS during the first month of age. This was achieved by raising two groups of fish that were not permitted exposure

to the flow generated by live *Artemia* prey. One group was fed dead *Artemia* (group 3, described in Results) and the LLS of the other group (group 4) was compromised throughout the rearing period. This was achieved by daily exposure to a neomycin solution (250 μmol l^{-1} neomycin sulfate for 45 min) prior to feeding with live *Artemia*. Both groups were consequently naïve to the flow created by live *Artemia* at the time that I performed feeding experiments at the juvenile age (30 dpf). Neomycin treatments ceased 2 days prior to these experiments to afford the time for regeneration of the LLS. This timing was selected because previous experiments showed that hair cells and responses to flow stimuli recover in zebrafish within 25 h of neomycin treatment (McHenry et al., 2009). Fish were only included in experiments if they exhibited routine swimming behavior and motivation to feed. In addition, fish treated with daily neomycin treatments were used only if they exhibited an escape in response to the flow of a pipette. I stained these fish with DASPEI to visually confirm the presence of neuromasts following our experiments.

Feeding experiments were recorded for 15 juveniles from each rearing regime and compared with the control (Group 1, described in Results) and lateral-line-compromised group (Group 2) of the same age. I tested for differences in capture and strike rates between treatment groups with a one-way ANOVA with post hoc comparisons (Tukey's HSD test). These measurements met the assumptions of a normal distribution (Kolmogorov–Smirnov, $P>0.05$) and homogeneity of variance (Levene's test, $P>0.05$). Capture probabilities were compared between treatment groups with a Kruskal–Wallis test, because these data did not meet the assumption of normality. A pairwise comparison, the Nemenyi test (with a Tukey distribution), was used to determine significant differences between groups.

Results

Changes in foraging with age

Zebrafish improved in their ability to feed on *Artemia* with monotonic increases in metrics of forage performance over the first month of age. Juveniles struck at prey with greater frequency and with a higher capture rate than larvae (Fig. 1). For example, the capture rate of juveniles (1.38±0.17 min^{-1}, mean±95% CI, N=15 at 30 dpf) was approximately an order of magnitude greater than that of 1-week-old larvae (0.11±0.03 min^{-1}, N=15 at 7 dpf; Fig. 1C). This was because the older fish would strike at greater frequency, with a strike rate (1.98±0.19 min^{-1}, 30 dpf) that was twice that of larvae (0.73±0.12 min^{-1}, 7 dpf; Fig. 1D), and each strike was approximately four times more likely to capture prey (strike probability: 0.18±0.09 at 7 dpf and 0.70±0.09 at 30 dpf; Fig. 1E).

I tested the role of flow sensing on foraging by compromising the LLS with a treatment of neomycin (Fig. 1A, B). This experimental manipulation had little effect when fish could see, as indicated by the lack of significant differences in the capture rate, strike rate, and capture probability when foraging under illumination (indicated by 95% confidence intervals, Fig. 1C–E). However, I did find substantial differences when fish foraged in the dark, particularly in individuals older than 15 dpf. For example, the control group at the juvenile age (30 dpf) exhibited a mean capture rate (0.82±0.25 min^{-1}, N=15) that was four times greater than that of fish with a compromised LLS (0.18±0.07 min^{-1}, N=15; Fig. 1F). In addition, both the strike rate (2.26±0.48 min^{-1}, N=15, Fig. 1G) and capture probability (0.37±0.09, N=15; Fig. 1H) of untreated juveniles were twice the values of the group with a compromised LLS (1.04±0.23

min^{-1}, 0.18±0.11, N=15; Fig. 1G). Therefore, flow sensing by the LLS appears to enhance feeding in the dark by eliciting fish to strike both more frequently and with greater effectiveness.

The role of the cranial lateral line in foraging

I tested the role of the cranial LLS on foraging in juvenile fish by chemically treating just the cranial neuromasts and leaving the posterior lateral line intact. I found that the foraging performance of fish with a compromised cranial system was indistinguishable from those with an entirely compromised LLS. In particular, the mean (±95% CI) capture rates of juveniles (25 dpf) without cranial neuromasts (0.07±0.05 min^{-1}, N=15) did not significantly differ from that of fish with an entirely compromised LLS (0.09±0.06 min^{-1}, N=15), but was significantly lower than that of both sham (0.47±0.11 min^{-1}) and untreated fish (i.e. 'with LLS', 0.53± 0.18 min^{-1}) (N=15, one-way ANOVA, $F_{3,59}$=16.2, P<0.001, Tukey's HSD, P<0.05; Fig. 2A). This result emerged despite the fact that the strike rate in fish without functional cranial neuromasts (1.13±0.34 min^{-1}) did not differ significantly from that of the sham group (1.63±0.29 min^{-1}; Fig. 2B). The strike rate of cranial-treated fish was also indistinguishable from that of fish lacking the entire LLS (0.58±0.18 min^{-1}), but significantly lower than that of control fish (1.95±0.36 min^{-1}, N=15 in each group, $F_{3,59}$=16.7, P<0.001, P<0.05; Fig. 2B). It is therefore unclear whether larvae strike less often when they lack only cranial neuromasts. However, our results do suggest that the cranial system contributes to the effectiveness of a strike. This was indicated by the capture probability of fish without cranial neuromasts (0.05±0.04), which was significantly lower than that of both the sham (0.25±0.05) and control groups (0.26±0.09, N=15), and did not differ from that of fish lacking the entire LLS (0.01±0.08, N=15, Kruskal–Wallis, H=22.8, P<0.01, pairwise comparisons, P<0.05; Fig. 2C).

I examined whether ontogenetic changes in the morphology of cranial neuromasts might account for the improvement in the ability of fish to forage in the dark. The mean (±95% CI) number of neuromasts in 15-dpf fish (41.8±3.3) was not significantly different from that of juveniles of 25 dpf (45.8±4.2) and 30 dpf (47.3±2.8, one-way ANOVA, $F_{2,44}$=2.51, P=0.093, N=15 in each group; Fig. 3). Measurements of the cupula of neuromasts in the cranial region revealed that neither its height nor diameter differed significantly with age (one-way ANOVA, d.f.=2, 26, P>0.05, N=9; Fig. 4B–D). I similarly found that the number of hair cells did not vary significantly with age for all cranial neuromasts (one- way ANOVA, d.f.=2, 44, P>0.05; Fig. 3B), with the exception of the fourth supraorbital (one-way ANOVA, $F_{2,44}$=4.30, P=0.02). At that site, larvae of 25 dpf (11.1±2.06) had significantly fewer hair cells than fish of 15 dpf (13.0±1.9, N=15) or 30 dpf (14.9±1.3, N=15, Tukey's HSD, P<0.05). This is not a pattern consistent with ontogenetic improvement in sensitivity of neuromasts. These results suggest that the morphology of the cranial LLS does not vary in a manner that could enhance the mechanical sensitivity between 15 and 30 dpf. Therefore, morphological changes cannot account for the improvement in foraging in the dark with age (Fig. 1G).

The effects of learning on foraging

I tested whether the improvement in foraging with age was a consequence of associative learning. Two groups of fish were raised under different feeding regimes to produce 30-dpf fish that were naïve to the flow generated by live *Artemia*. One group was fed dead *Artemia* (Group 3 in Fig. 5) and the other was fed live food but was raised with a compromised LLS through daily neomycin treatments (Group 4 in Fig. 5). Fish in the compromised group were permitted to regenerate their LLS prior to our measurements of foraging performance. I performed foraging

experiments in the dark on these naïve groups with the same experimental design as the fish that were exposed to the flow of prey. I found that fish that were naïve to the flow of *Artemia* were less effective at foraging than fish raised with exposure to flow. For example, fish raised on dead *Artemia* (Group 3: 0.41±0.13 min^{-1}; Fig. 5A) and those with a compromised LLS (Group 4: 0.27± 0.13 min^{-1}) exhibited less than half the capture rate of the control fish (Group 1: 0.82±0.25 min^{-1}), which was a significant difference (one-way ANOVA, $F_{3,59}$=12.5, P<0.001, Tukey's HSD, P<0.05). Both of the naïve groups (Groups 3 and 4) were statistically indistinguishable from the fish that were unable to sense flow while foraging in the dark (Group 2 in Fig. 5) in terms of capture rate (one-way ANOVA, $F_{3,59}$=9.65, P<0.001, Tukey's HSD, P<0.05; Fig. 5B) and capture probability (Kruskal–Wallis, H=15.7, P<0.01, pairwise comparisons, P<0.05; Fig. 5C). However, fish raised on dead *Artemia* (Group 3) showed intermediate values in both strike rate and capture probability (Fig. 5B,C). Therefore, larvae may gain some advantage to being raised with a functional LLS, even when naïve to the flow generated by *Artemia*. These results are consistent with the hypothesis that larval fish improve in their ability to forage in the dark (Fig. 1F–H) because they learn to associate *Artemia* with the flow generated by this prey for propulsion.

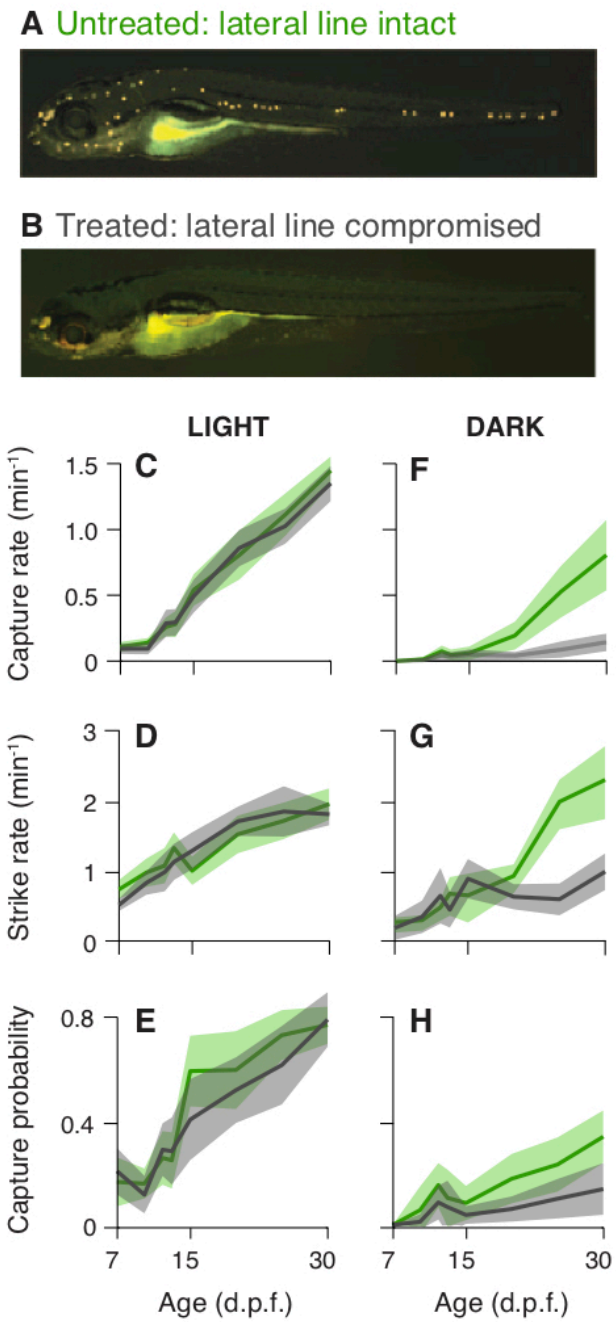

Fig. 1. Effects of the lateral line system in *Danio rerio* on foraging with age. (A) The hair cells of the superficial neuromasts of the lateral-line system (LLS) are stained with DASPEI under fluorescent illumination. This causes each receptor to appear as a yellow point along the body of an untreated larva (5 dpf) with a functional LLS. (B) DASPEI staining fails to reveal any lateral line hair cells in a larva (5 dpf) exposed to neomycin sulfate. (C–H) The results of experiments of fish of varying age that foraged on *Artemia* under (C–E) illuminated and (F–H) darkened conditions are presented through three performance metrics. The measurements (mean±95% CI) of capture rate (C,F), strike rate (D,G) and capture probability (E,H) are shown (N=15 fish at each age).

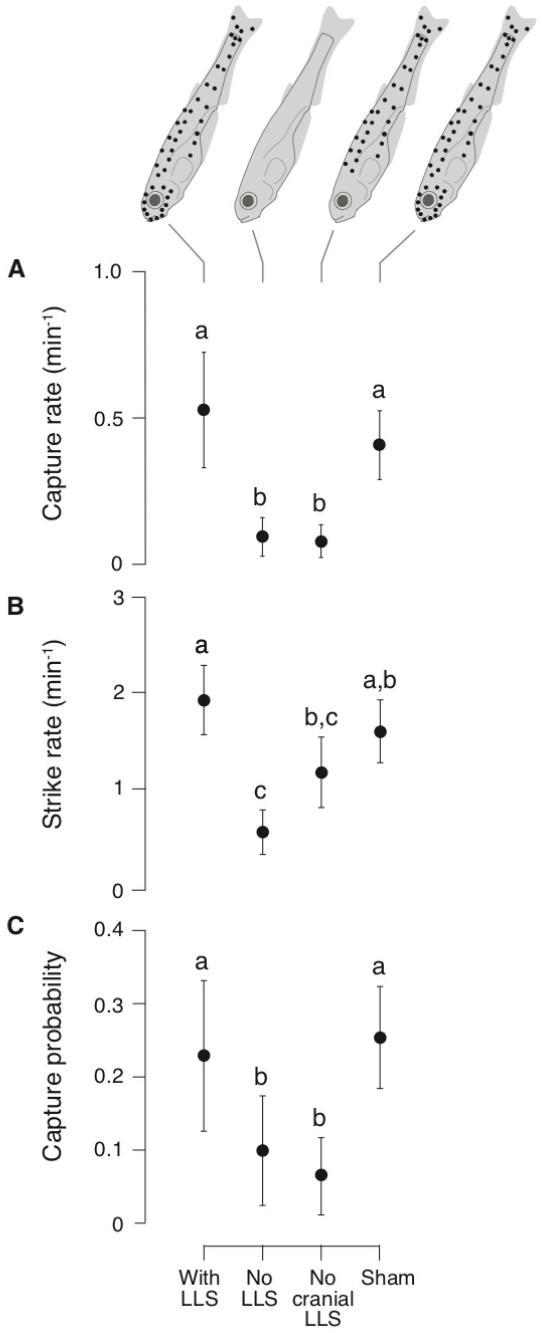

Fig. 2. Effects of the cranial lateral line on foraging. The results of foraging experiments for four treatment groups are reported (mean±95% CI) in terms of the (A) capture rate, (B) strike rate, and (C) capture probability of juvenile zebrafish (25 dpf) foraging on *Artemia*. The groups consisted of a control with an untreated LLS ('with LLS'), a group where each fish had its entire LLS compromised by exposure to neomycin sulfate ('no LLS'), another where just the cranial lateral line was compromised ('no cranial LLS'), and a sham group that was handled in the same manner as the 'no cranial LLS' group. Different letters indicate significant differences between groups (N=15 fish in each group).

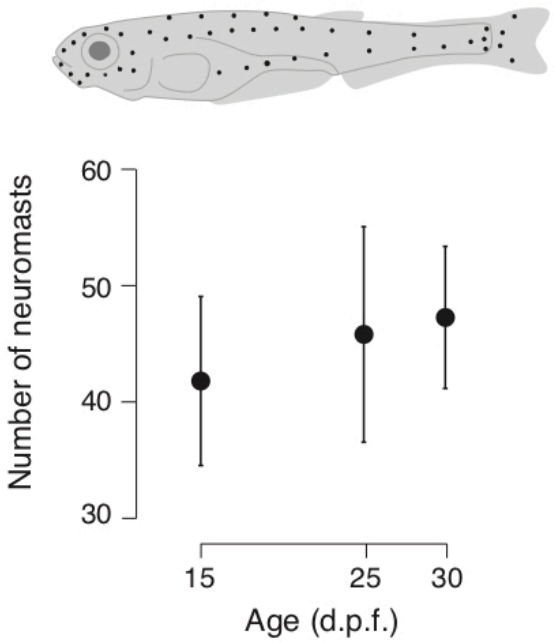

Fig. 3. Total number of neuromasts with age. The number of neuromasts (mean±95% CI) on the head and body in lateral view of zebrafish (15 to 30 dpf), which did not differ significantly among ages (one-way ANOVA, P=0.09, N=15 fish at each age).

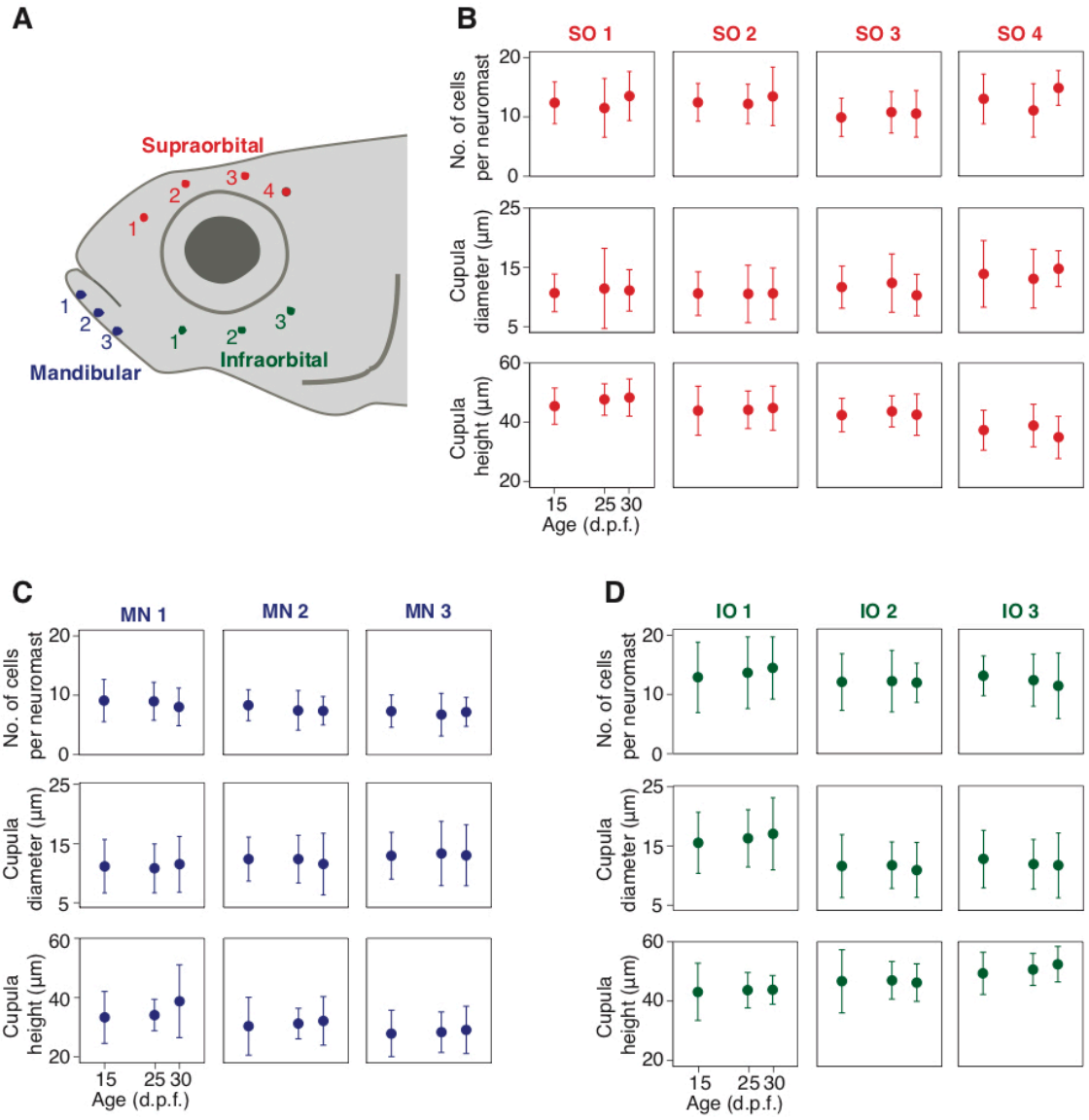

Fig. 4. Morphology of cranial neuromasts with age. (A) Illustration of the locations of cranial neuromasts measured in zebrafish. (B–D) Morphometric features measured for the (B) supraorbital, (C) mandibular, and (D) infraorbital neuromasts among zebrafish at 15, 25, and 30 dpf (mean±95% CI, N=9, at each age). For each neuromast, I measured the number of hair cells and the diameter and height of the cupula.

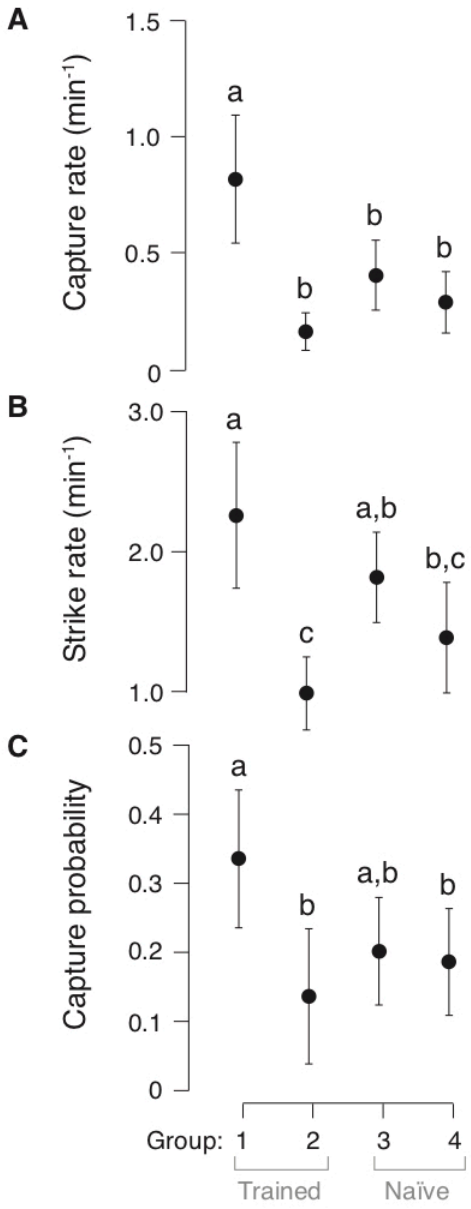

Fig. 5. Effects of learning on foraging performance in the dark. The effects of learning were addressed through measurements of foraging performance in the dark for four groups of juvenile zebrafish (30 dpf, N=15 for each group) that were raised under distinct conditions. Groups 1 and 2 were raised on live *Artemia* and were thereby exposed to the flow generated by prey. Group 1 serves as a control because the LLS was not manipulated, whereas foraging in Group 2 was performed on fish with a LLS compromised by exposure to neomycin. The other two groups were naïve to the flows created by *Artemia* by the time of the foraging experiment. This was achieved by raising fish that either were fed dead *Artemia* (Group 3) or were exposed to neomycin daily to compromise the LLS, (Group 4). Values (mean±95% CI) of (A) capture rate, (B) strike rate, and (C) capture probability are shown with different letters indicating significant differences between groups (Tukey's HSD).

Discussion

Our results offer new insight into the role of the LLS in the foraging of larval zebrafish. I found that: (1) foraging in the dark improves with age, (2) the cranial neuromasts play a major role in this foraging, and (3) the improvement in foraging with age is an effect of larvae learning to sense the flow of prey. These results have emerged from the results of observations and manipulative experiments that used a variety of techniques.

Foraging in the dark improves with age

Our experiments allowed us to consider the role of the LLS when prey are visible. I observed an order-of-magnitude increase in capture rate over one month of age in foraging under illumination (Fig. 1C). This increase was generated by fish striking with greater frequency (Fig. 1D) and higher capture probability (Fig. 1E). None of these trends were adversely affected when I removed the ability of larvae to sense flow. When performing similar experiments, Westphal and O'Malley (2013) measured a subtle (∼25%) decrease in feeding rate in older larvae (15 and 30 dpf). Nonetheless, it can be concluded that the LLS is not necessary for foraging when guided by vision.

In contrast, I found that flow sensing plays a major role in foraging in the dark. This was indicated by the substantial reductions in performance that I observed when I compromised the LLS (Fig. 1F–H), which is consistent with previous results (Westphal and O'Malley, 2013). The effect of this experimental treatment was most acute on fish older than 15 dpf (Fig. 1F), which struck at prey at a lower frequency (Fig. 1G) and less accurately (Fig. 1H) without the aid of the LLS. Therefore, the assistance offered by the LLS in foraging increases with the age of zebrafish.

Cranial neuromasts are important for foraging

I found that the ability to sense the flow of prey is largely facilitated by cranial neuromasts. Fish retaining a functional posterior lateral line, but compromised cranial system, exhibited a capture rate that was indistinguishable from that of fish lacking all functional neuromasts (Fig. 2A). Without the aid of flow sensing at the head, fish would strike less often (Fig. 2B) and with lower accuracy (Fig. 2C) than control and sham groups. These results are consistent with descriptions of how juveniles change their orientation and strike at *Artemia* that come in close proximity to the head, without contacting the surface of the body (Westphal and O'Malley, 2013). Therefore, the flow detected by cranial neuromasts appears to prompt fish to both initiate feeding and align a strike toward the prey. These results do not preclude a role for the posterior lateral line, which is considered to play a role in predator evasion (Stewart et al., 2013, 2014). I found that fish foraging without the entire LLS would strike less often than those lacking just the cranial system (Fig. 2B), but the capture probability was indistinguishable between these groups (Fig. 2C). Therefore, the posterior lateral line may serve a minor role in stimulating foraging, but it does not enhance the effectiveness of a strike.

I found no evidence that change in the morphology of neuromasts enhances flow sensing with age. Our analysis focused on the cranial neuromasts, because of their above-mentioned prominent role in foraging. These neuromasts did not increase in number between 15 and 30 dpf (Fig. 3), which is the period where I found the largest increase in foraging performance (Fig. 1). In addition, the size and shape of the neuromasts did not change in any way that would serve to enhance sensitivity (Fig. 4). This finding was based on our measurements of the number of hair cells and the dimensions of the cupula, which are the major features that determine the mechanical sensitivity of a superficial neuromast (McHenry et al., 2008; van Netten and

McHenry, 2013). It is surprising that these features did not vary with age, because previous studies suggested that this period coincides with a proliferation in the number of cranial neuromasts (Nuñez et al., 2009) and the advent of canal neuromast development at 22 dpf (Webb and Shirey, 2003). These changes are likely to impact the role of the cranial LLS, but they correspond to developmental transformations that apparently occur after the ages that I considered. The discrepancy between present and past studies is likely due to differences in the rearing conditions (Schilling, 2002). In support of this interpretation, our juveniles (30 dpf) were substantially shorter in body length (~9.0 mm) than juveniles in at least one of these prior studies (~10.4 mm) (Webb and Shirey, 2003).

Larvae learn to sense flow

I tested the hypothesis that larvae improve in their ability to forage in the dark (Fig. 1F) as a consequence of learning. The larvae reared for our experiments were fed live *Artemia* daily under illuminated conditions. According to our hypothesis, larvae acquired an association between the flow generated by the swimming of *Artemia* and the reward of ingested prey. Therefore, larvae were capable of recognizing the flow of *Artemia* without vision when I performed a foraging experiment in the dark. This hypothesis predicts that larvae raised under conditions that prohibit the opportunity to associate a flow stimulus with feeding will be as ineffective at foraging in the dark as larvae lacking the LLS. This was indeed what I found. Larvae that were either raised with a daily treatment of neomycin or were fed dead *Artemia* exhibited a capture rate that was indistinguishable from those with a compromised LLS (Fig. 5A). I therefore interpret the ability of larvae to improve in their feeding in the dark with age (Fig. 1F) to be a consequence of associative learning.

Our results are consistent with previous studies on learning in zebrafish. Under classical conditioning, adult zebrafish learn to direct their swimming in response to visual stimuli (e.g. Darland and Dowling, 2001; Sison and Gerlai, 2010; Bianco et al., 2011) and to forage in response to synthetic chemicals (Braubach et al., 2009). Young larvae (6–8 dpf) can similarly be trained to exhibit tail-flicking behavior in response to light by pairing it with touching by a probe (Aizenberg and Schuman, 2011). The ability to perform associative learning increases with age. In experiments that used swimming in response to visual cues, Valente et al., (2012) found larvae younger than 4 weeks old to be unresponsive to classical conditioning, but to respond to operant conditioning by electric shocks as young as 3 weeks old. Our results suggest that larvae may begin to learn by 15 dpf when offered the reward of prey.

Our results are significant to the advancement of the understanding of the larval ecology of fishes and the neurophysiology of learning. Fish capable of learning to identify flow can forage when vision is compromised, such as in dark or turbid waters. This suggests that the sensory systems of fishes are sufficiently plastic that they may generally be recruited for essential functions. Such plasticity is likely to permit foraging under situations that challenge competitors and predators. This ability to learn has been demonstrated in zebrafish, which are an exciting model system for neurophysiology because of the techniques of functional imaging and optogenetics (e.g. Fetcho and Higashijima, 2004; Portugues et al., 2013). Through these approaches, it is increasingly possible to examine the physiological basis of learning.

CHAPTER 2: CANAL NEUROMASTS ENHANCE FORAGING IN ZEBRAFISH

Introduction

A broad diversity of aquatic animal taxa sense water flow with mechanoreceptors on the surface of the skin. Such a receptor generally includes an elongated structure that extends into the water, where it is deflected by hydrodynamic forces (Dijkgraaf, 1963). This motion is transduced into a nervous signal by mechanosensory cells anchored within the skin. In fishes (Dijkgraaf, 1963; Coombs and Montgomery, 1999) and amphibians (Scharrer, 1932), these receptors are known as superficial neuromasts (SNs), and they include a cluster of hair cells that are deflected by flow through their coupling to an extracellular structure, known as the cupula. Similar receptors (perhaps homologous) are found among cnidarians (Arkett et al., 1988), tunicates (Bone and Ryan, 1978), echinoderms (Cobb and Moore, 1986), and cephalopods (Budelmann and Bleckmann, 1988), and analogous structures are present in marine arthropods (Lenz and Yen, 1993; Fields and Weissburg, 2004), and insects (Sane and McHenry, 2009). A SN is sensitive to the flow velocity of most relevant frequencies because its deflections are created by viscous drag (van Netten and McHenry, 2013).

The lateral line of teleost fishes is unique among animals because it also includes a second type of receptor, the canal neuromast (CN). A CN is also a hair-cell mediated flow receptor, but its hemispherical cupula resides within a canal beneath the body's

surface. These canals are generally opened to the surface via pores that induce flow through the canal with a difference in pressure. As a consequence, CNs respond to spatial gradients in pressure, such as those generated by an accelerating flow field (Denton and Gray, 1983). Due to the distinct sensitivity of SNs and CNs, the fish lateral line is described as possessing two submodalities of flow sensing (Coombs and Montgomery, 1999) that exhibit contrasting responses to flow stimuli. Although CNs are considered to be more sensitive to an oscillating flow stimulus (van Netten and McHenry, 2013), it is not clear how a fish benefits from having CNs in addition to SNs. Therefore, the aim of the present study was to test whether CNs enhance the ability of fishes to forage in the dark.

The role that CNs play in behavior has perplexed biologists since their discovery. It is clear that CNs are not necessary for the lateral line system to mediate some behaviors. For example, larval fishes generally do not possess CNs, yet their lateral line mediates escape responses to an approaching predator (Stewart et al., 2014; Nair et al., 2017) and rheotaxis (Oteiza et al., 2017). In some lineages, CNs have been secondarily lost (Wark and Peichel, 2010), with no qualitative deficits in behavior. Nonetheless, CNs have been retained among a broad diversity of fishes, which suggests that this submodality offers some functional benefit. Perhaps the most compelling case for the value of CNs is offered by the prey localization behavior in the nocturnal foraging of the mottled sculpin. Hydrodynamic models of the oscillating flow generated by a prey (Kalmijn, 1989) successfully predict the nervous patterns generated by CNs along the length of the body (Coombs and Montgomery, 1999) and experimental ablation of SNs showed no significant effect on this behavior (Coombs et al., 2001). This essential role of the CNs applies to other species of fishes that are similar in size (Ćurčić-Blake and van Netten, 2006; Goulet et al.,

2008). This research suggests that the ability to localize a stimulus requires an array of CNs that are distributed along the trunk is comparable in length as the distance to the stimulus (Jannsen, 1997). In addition, the dipole model that predicts the lateral line responses is inviscid and therefore neglects the boundary layer flows that excite SNs. It is therefore unclear how CNs play a role in the foraging behavior of smaller animals and whether SNs might play a larger role in foraging in a different hydrodynamic regime.

The present study investigated the role of CNs in foraging behavior by comparing adults that have CNs to juveniles that do not. This work was performed on zebrafish (*Danio rerio*, Hamilton, 1922), which grow into adulthood at around a centimeter in length (Singleman and Holtzman, 2014), which is about an order of magnitude smaller than the mottled sculpin (Brown, 1981) and therefore presumed to localize prey at a different hydrodynamic regime than considered previously. Despite possessing a lateral line with only SNs, juvenile zebrafish forage on zooplankton in the dark, guided by flow stimuli (Westphal and O'Malley, 2013; Carrillo and McHenry, 2016). In a pilot study, I discovered that this behavior may be elicited in zebrafish with the flow generated by a vibrating rod, similar to what has been observed with a relatively large vibrating sphere in larger species, like the sculpin (Coombs and Janssen, 1990). I compared the bite rate elicited by this stimulus over a range of frequencies in juveniles and adults and compared these behavioral frequency responses to predictions of the frequencies responses of CNs and SNs, based on biophysical modeling. In addition, I measured the distance at which these fishes responded to the stimulus, visualized this flow field, and modeled the responses of CNs and SNs to this flow. These observations were supplemented with experimental manipulations that tested the role of SNs and CNs in adults. These approaches combined

to offer a comprehensive view of the role of CNs for foraging in the dark.

Materials and Methods

Animal Care

Zebrafish were reared from wild-type colonies housed in a flow-through system (Aquatic Habitats, Apopka, FL, USA) maintained at 27.5°C. Zebrafish were raised in tanks (3 L) connected to a recirculating system and were fed pellets (Larval AP100 and AP400, Ziegler Bros Inc., Gardens, PA, USA) daily. Zebrafish were grown to two age groups: juveniles (30 days post-fertilization, dpf, mean standard length and range: 8.67, 7.56 - 9.35 mm), which possessed SNs only, and adults (90 dpf, mean standard length and range: 17.13, 15.2-18.42 mm), which possessed both SNs and CNs. All rearing and experimental protocols were conducted with the approval of the Institutional Animal Care and Use Committee at University of California, Irvine (protocol #AUP-17-12; #2554-2005).

Behavioral experiments

I used a vibrating rod to stimulate foraging in zebrafish. The enlarged end of the rod (dia.=300 μm) was formed by melting a bead of glass at the distal end of a microcapillary tube (dia.=200 μm). Oscillations in the position of the rod were performed with a piezoelectric actuator (P-840.60, Physik Instrumente, Karlsruhe, Germany) that deflected a steel shim (0.15 mm thick) that was attached to the base of the rod (Fig. 1A). This actuator was operated with a closed-loop controller (PI Amplifier E-501.00, Physik Instrumente) that generated sinusoidal oscillations at a fixed amplitude of displacement (200 μm) over a frequency range from 2 Hz to 100 Hz, as dictated by a function generator

(AGF3021, TekTronix, Beaverton, OR, USA). The distal end of the rod was submerged to a depth of 3.0 mm below the surface of the water for all experiments.

I tested the responsiveness of the fish's behavior to different frequencies to see whether adults (CN + SN) are more sensitive to high-frequency stimuli than juveniles (SN only). This behavioral frequency response was performed by measuring the rate at which groups of fish would bite at the vibrating rod with video recordings in the dark. These experiments were conducted in a cylindrical tank (dia.= 100 mm, 80 mL of aquarium-system water, 24°C) with no visible light. I added the scent of food (ground pellets) mixed into the tank water to motivate the fish to forage. In the interest examining behavior in response to steady-state oscillatory flow, the rod positioned at the center of the tank was driven to oscillate for 30 s before I commenced video-recording for the flow field to establish steady-state conditions. The camera (FASTCAM, 1024PCI, Photron, San Diego, CA, USA, 4 x 4 cm field of view, 512 x 512 pixels, at 30 frames s^{-1}) recorded from below using a mirror positioned at a 45 deg angle. An array of infrared LEDs (850 nm) were placed above to video-record the fish with transmitted illumination in the absence of visible light (Fig. 1A). From these videos, I recorded the number of feeding strikes within a 2-min period. This experiment was repeated for each group of fish at eight stimulus frequencies, chosen in a randomized order and interrupted with a 30-min resting period between experiments to minimize habituation. Seven groups of both adults and juveniles were exposed to one set of 8 frequencies that spanned equal intervals at a 10-based log scale (i.e. 2.0, 3.5, 6.1, 10.7, 18.7, 32.7, 57.2, and 100 Hz), as well as a control where the rod did not vibrate. Seven other groups were exposed to frequencies interspersed between these values (i.e. 13.3, 17.1, 21.9, 28.3, 36.4, 46.8, 60.3, and 72.6 Hz). Together,

experiments were performed for 14 groups of juveniles and 14 groups of adults, with each group consisting of 5 individuals.

In another set of experiments, I tested the behavioral sensitivity of flow sensing by measuring the distance at which fish responded to the vibrating rod in the dark. I recorded responses to the vibrating rod with high-speed video recordings (1240x1240 pixel, 24 x 24 mm field of view at 1000 frames s^{-1}, FASTCAM, 1024PCI, Photron) under magnified optics (KC VideoMax S lens with an Achrovid 5x objective, INFINITY, Boulder, CO, USA) for individuals in a petri dish (dia.= 60 mm, 15 mL of water, at a height of 12 mm, at 24.0 ˚C), with the rod positioned in the center (Fig. 1B). The fish were motivated to forage by fasting them for three days and exposing them to the scent of ground food pellets mixed into the water. Each fish was exposed to the rod vibrating at three frequencies (20, 50, and 80 Hz) in a random order. I determined where the fish responded to flow with an unconditioned behavioral response, eye vergence, previously discovered in zebrafish larvae (Bianco et al., 2011; Patterson et al., 2013), which I verified in adults and juveniles. Before a fish approaches a prey and strikes at it, vergence occurs by the eye rotating anteriorly, even when foraging in the dark. I identified the onset of vergence by measuring the angular orientation between the eyes. This was achieved with a custom program developed in MATLAB (v. 2015b with the image processing toolbox, Mathworks, Natick, MA, USA). This program succeeded in using image registration to stabilize the video recording for a region of interest that included the head. I then described the orientation of the eyes using a fit-best for an elliptical shape and then calculated the angle, termed the vergence angle (θ), was calculated as that between the major axes of the two ellipses (Fig. 1C). Vergence exhibited a rapid change in this angle,

which was maintained up to when the fish would strike at the rod (Fig. 1D). The response distance was measured from the center of the eyes to the center of the rod axis at the moment that vergence was initiated.

Comparisons of our behavioral measurements between juveniles, adults, and adults with experimentally-manipulated lateral lines (described below) were performed with non-parametric statistics. These tests were chosen in favor of conventional statistics because I found that many of our measurements were not normally-distributed (Kolmogorov-Smirnov test, $P < 0.01$) and could not be normalized with standard transformations. Comparisons between juveniles and adult groups were performed using separate Kruskal-Wallis tests. This included comparing measurements of bite rate at different frequencies and response distance using RStudio (version 1.0.136). Pairwise comparisons with Nemenyi tests (using a Tukey distribution approximation) were used to determine significant differences between groups for each set of experiments.

Experimental manipulation and morphometrics of the lateral line

I measured response distance in experimentally-manipulated adult fish, as an additional test of the role of the lateral line in foraging. The first manipulated group tested the role of all cranial neuromasts by compromising neuromasts in that region and leaving those in the rest of the body intact (a group denoted 'No cLL'). This was achieved by exposing only the head of an anesthetized adult fish to an ototoxic solution of 2.5 mM neomycin sulfate (Fisher BioReagents, FairLawn, NJ, USA) for 30 min. The trunk neuromasts were protected from this treatment by embedding the body in a block of 6% agar (low-melting point agarose, Fisher Scientific, Fair Lawn, NJ, USA). I first encased the whole body in molten agarose that was heated to 32.0°C and then I solidified the material by placing

this preparation in a 27.5°C bath. Once set, the agar around the head was removed with a scalpel, and the head was exposed to the neomycin solution (buffered pH=7.0 in aquarium water, under aeration). After a 30-min exposure period, the fish were removed from the agar and allowed to recover in a petri dish with aquarium water for 30 min. In another group ('CN only'), I tested the role of cranial SNs by applying an ototoxic paste to the head that compromised SN hair cells and left the CNs unaltered. The paste consisted of 1.5% agarose heated to 60.0°C), mixed with a solution of 10 mM neomycin sulfate. The paste was applied after cooling to 36.0°C with a paint brush over the surface of the head of an anaesthetized fish (buffered MS-222; Finquel, Argent Chemical Laboratories, Remond, WA, USA, 0.001 g L^{-1}, under aeration). After a 10-min exposure period, the paste was removed with a cotton swab and the fish allowed to recover in a petri dish with aquarium water. Treated fish were only used for experiments if they exhibited normal swimming and motivation to feed after treatment.

The efficacy of experimental treatments was determined by visualizing neuromast hair cells with a fluorescent stain. This vital stain, DASPEI ((2-(4-(dumethylamino)styryl)-N-ethylpyridinium iodide, Invitrogen, Eugene, OR, USA), differentially stains hair cells with an intensity that is positively related to the sensitivity of mechanotransduction (Harris et al., 2003; Van Trump et al.,2010). I applied DASPEI by placing fish in a 0.02% solution for 10 min, which is a sufficient duration for the stain to infiltrate the hair cells of SNs and CNs. Stained neuromasts were photographed with a digital camera (AxioCam HRc, Carl Zeiss, Thornwood, NY, USA) connected to a stereomicroscope (225X, Zeiss Discovery V.20, Carl Zeiss) that included a fluorescent illuminator (120W Mercury Vapor Short Arc, X-Cite series 120q, Lumen Dynamics,

Mississauga, ON, CA) and GFP filter set. Four CNs (two supraorbitals and two infraorbitals neuromasts) and the four SNs closest to each CNs were photographed to compare the relative fluorescence intensity of individual neuromasts in treated and control fish. Relative intensity was determined from photographs as the mean pixel intensity of treated neuromasts, divided by the intensity of the same neuromast in control fish (scripted in MATLAB). These measurements were performed for all fish treated with neomycin at the conclusion of experiments. The images of neuromasts that were stained with DASPEI were used for morphometrics. We measured the linear the dimensions of the bundle of hair cells in cranial SNs and CNs from images of untreated fish. The size of this region was assumed to approximate a circular (in SNs) or elliptical (in CNs) base of the cupula. Measurements were performed with Fiji software (version 1.0, ImageJ, Madison, WI, USA). The canal width were also measured using Fiji software from the images of the supraorbital CNs, in which the canal was clearly visible.

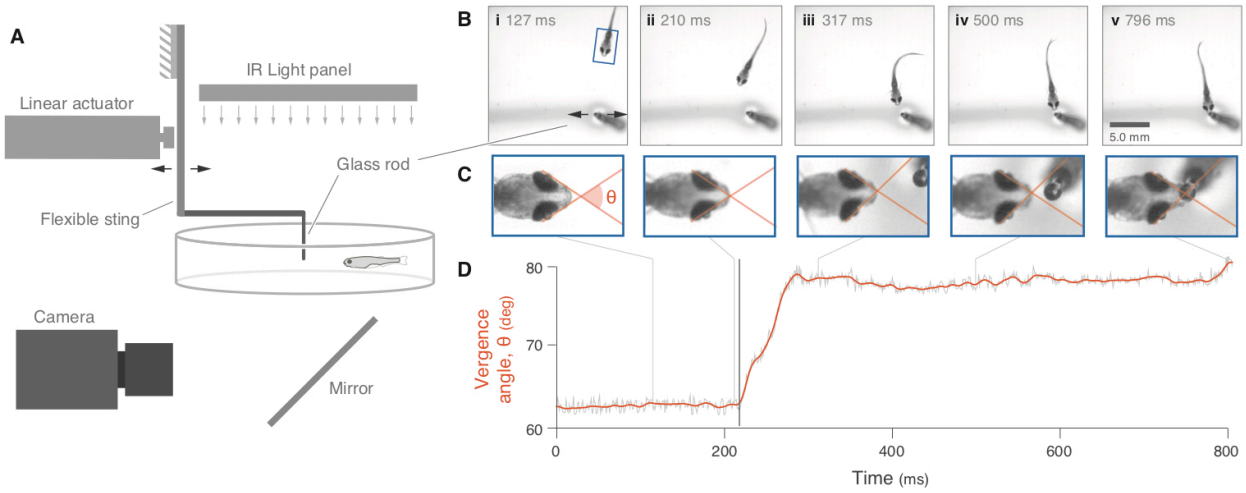

Figure 1: Experimental setup for behavioral experiments. (A) The behavioral responses of zebrafish to a vibrating rod were recorded with high-speed videography in the absence of visible light. The bodies of fish were visualized with an array of IR LEDs positioned above the tank that contained the fish. (B) A sample recording of a juvenile that approached and struck at the vibrating rod. (C) I performed an image analysis that stabilized the head of the animal and permitted measurement of the relative orientation of the eyes, expressed by the vergence angle (θ). (D) Before a strike, the vergence angle (orange curve is a filtered version of the raw measurements in gray) increased and maintained a relatively high value while approaching the vibrating rod. I used the position of the head of a fish at the moment of the onset of vergence (heavy gray line) to measure the response distance (Fig. 5).

Results

Behavioral Experiments

The feeding responses of adult and juvenile zebrafish to a vibrating rod varied with the stimulus frequency. At frequencies below 10 Hz, the median bite rate of adult fish ($\tilde{x}$=1.44 min^{-1}, where $\tilde{x}$ is the median value and the range is 0.72–1.89 min^{-1}, N=5) was indistinguishable from that of juveniles ($\tilde{x}$=1.17 min^{-1}, 0.50–1.33 min^{-1}, N=5, Fig. 2A,B). However, bite rate increased three-fold at higher stimulus frequencies in adults ($10<f<50$ Hz: $\tilde{x}$=3.50 min^{-1}, 1.44–3.83 min^{-1}, N=8; $50<f<100$ Hz: $\tilde{x}$=3.75 min^{-1}, 3.33–4.33 min^{-1}, N=4). A more subtle increase was observed in juveniles ($10<f<50$ Hz: $\tilde{x}$=2.17 min^{-1}, 1.17–2.94 min^{-1}, N=8: $\tilde{x}$=1.97 min -1, 1.11–3.28 min^{-1}, N=4), to a degree that the bite rate at 100 Hz was statistically-indistinguishable from that of low-frequency stimuli (Kruskal-Wallis, $H(7)=7.00$, P=0.43, Fig. 2B). Therefore, the responsiveness of zebrafish to high-frequency stimuli was significantly more pronounced in adults than juveniles (Fig. 2A–B). Similar patterns of frequency response were found in our predictions of lateral line sensitivity, discussed below (Fig. 2C). Experimental manipulations of the lateral line provided the means for us to test whether the enhanced sensitivity to flow of adult zebrafish may be attributed to the development of CNs (Fig. 3). Using relative fluorescence (i.e. relative to the same neuromasts in the control) as an indication of hair cell function, our treatment of an ototoxic paste to the cranial region ('CN only') succeeded in compromising the functioning of SNs ($\tilde{x}$=0.11, 0.07–0.16 relative fluorescence, N=27), while leaving CNs largely unaltered ($\tilde{x}$=0.76, 0.63–30.96, N=27, Fig. 3D) in adult fish. Treating the cranial region with an ototoxic solution ('No cLL'), by contrast, compromised both CNs ($\tilde{x}$=0.16, 0.10–0.17, N=18) and SNs ($\tilde{x}$= 0.13, 0.07

–0.14, N=18) in adults. Therefore, these treatments provided an opportunity to test whether foraging is mediated by the cranial lateral line and whether the CNs are sufficient to exhibit the high behavioral responsiveness of adults.

I examined whether these manipulations affected the probability that the fish exhibited vergence (Fig. 1C–D) in response to the vibrating rod. This probability in both adults (0.83±0.083, ±95% confidence interval, N=145) and juveniles (0.80±0.069, N=115) was about 80% when exposed to our artificial stimulus among all three stimulus frequencies (20, 50, and 80 Hz, Fig. 4). The probability of vergence was not significantly altered (Kruskal-Wallis, $H(13)=17.46$, $P=0.18$) in adults with compromised SNs in the cranium ('CN only': 0.77±0.094, N=94). However, adults entirely lacking a functional cranial lateral line showed vergence in less than one-fifth of experiments ('No cLL': 0.18±0.081, N=78), which was a highly-significant difference (Kruskal-Wallis, $H(3)=27.21$, $P<0.001$, pairwise comparisons, $P<0.05$). In addition, fish in this group would bite at the rod only after contacting it with their fins, barbs, or body surface. Therefore, cranial neuromasts are necessary for vergence without tactile stimuli and cranial CNs are sufficient for a high probability of vergence.

The distance at which fish responded to the vibrating rod was found to vary among some of our experimental groups. This measurement was taken from the position of the center of a fish's head at the time when they exhibited vergence (Fig. 1C–D) for stimuli at 20, 50, and 80 Hz (Fig. 5A). At a low stimulus frequency (20 Hz), adults ($\tilde{x}$= 4.55 mm, 1.29–11.38 mm, N =43) exhibited vergence (Fig. 1–D) at a 60% greater distance than juveniles ($\tilde{x}$=2.79 mm, 0.85–7.93 mm, N=30, Fig. 5), which was statistically-significant (Kruskal-Wallis, $H(5)=48.23$, $P<0.001$, pairwise comparisons,

$P<0.05$, Fig. 5B). This difference was more pronounced at higher stimulus frequencies. At 50 Hz, adults ($\tilde{x}$=7.25 mm, 1.41–12.77 mm, N=38) responded by more than twice the distance of juveniles ($\tilde{x}$=3.52 mm, 1.02–8.22 mm, N=31). At 80 Hz, adults ($\tilde{x}$=7.03 mm, 1.13–11.28 mm, N=39) responded at nearly three times the distance of juveniles ($\tilde{x}$=2.60 mm, 0.87–10.63 mm, N=31). All of these differences were highly significant (Kruskal-Wallis tests, $P<0.01$, pairwise comparisons, $P<0.05$, Fig. 5). However, the response distance was not significant between adults with compromised SNs ('CN only') and unaltered fish ('SN + CN', Kruskal-Wallis tests, $P>0.32$, Fig. 5). Therefore, cranial SNs are not necessary for the high behavioral sensitivity shown in adults.

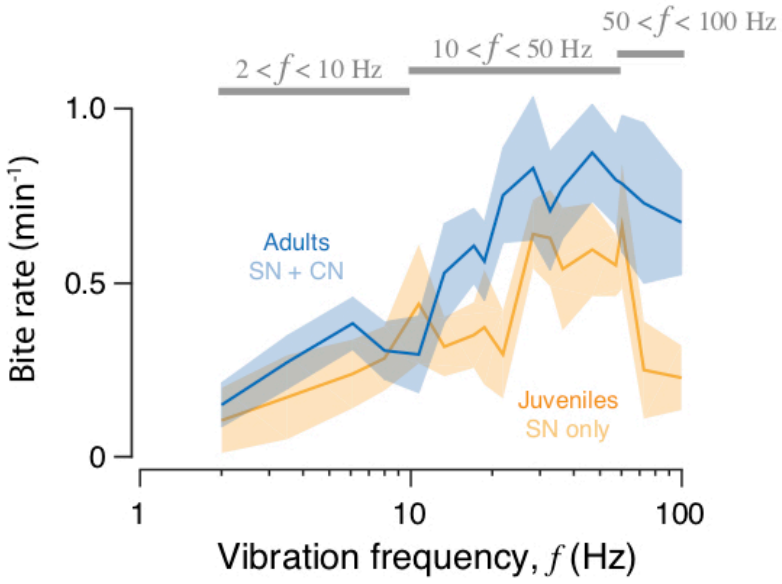

Figure 2: The behavioral frequency response to a vibrating rod. (A) The bite rate is the frequency by which an individual struck at the vibrating rod placed in the center of a petri dish (Fig. 1A). These experiments were performed with 14 groups of 5 adult (in blue) and juvenile (in orange) fish ($N = 7$).

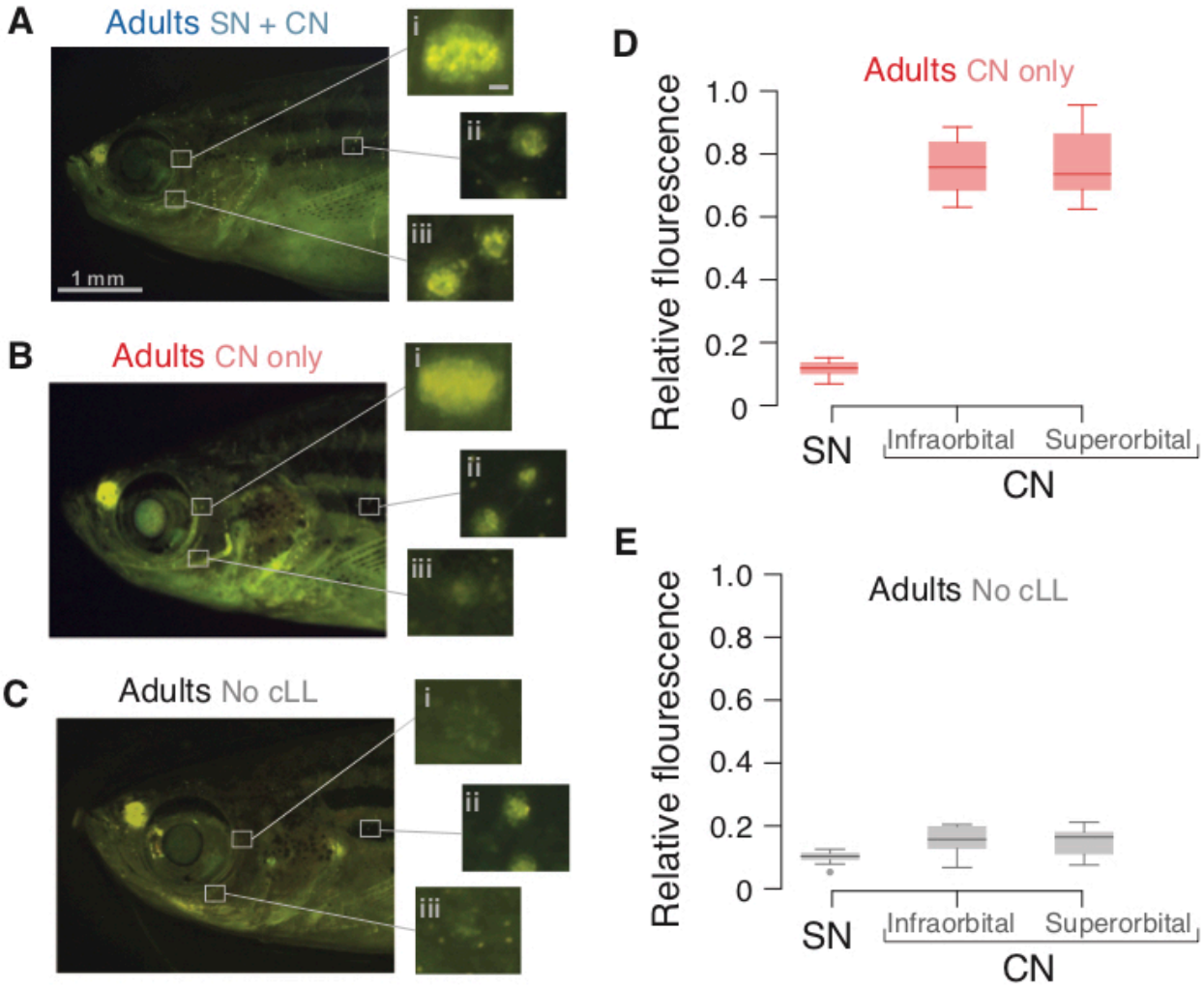

Figure 3: Experimental manipulation of the lateral line system in adult zebrafish. (A–C) Images of the fluorescence of lateral-line hair cells were used to assess the effectiveness of the manipulations. The inset images show hair cells for (i) a single supraorbital-canal neuromast, and pairs of superficial neuromasts in the (ii) trunk and (iii) cranial regions) (10 µm scale bar length). (A) A representative control animal showed a high level of fluorescence in the hair cells of all three types of neuromast, indicating that they were all functional. (B) Through the application of an ototoxic paste in the 'CN only' group, the SNs in the cranial region (iii) were compromised. The CNs in the cranium (i) and the SNs in the trunk were qualitatively similar to the control. (C) In contrast, exposure of the entire head to an ototoxic solution ('No cLL') compromised both types of neuromast in the cranial regions, while leaving the trunk SNs (ii) unaltered. These qualitative results were supported by measurements of fluorescence, expressed relative to the control in (D) 'CN only' ($N = 27$) and (E) 'No cLL' ($N = 18$) treatment groups (see text for statistics). Each rectangle in the boxplot extends from the first to third quartiles, with a center line at the median value and error flags that span the range.

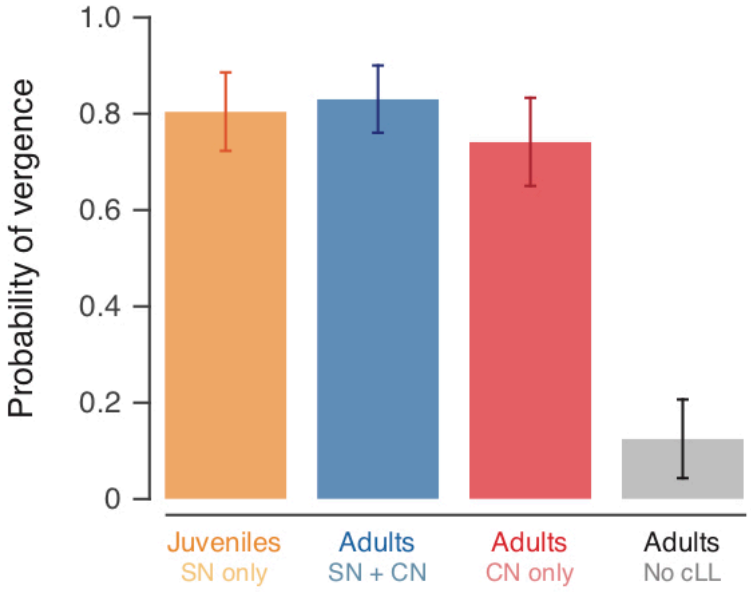

Figure 4: The probability of exhibiting vergence for treatment and age groups. Juveniles (in orange, *N*=115), adults (in blue, *N*=145), and adults with compromised cranial SNs ('CN only', in red, *N*=94) all exhibited a statistically-indistinguishable probability of vergence of around 80% (±95% confidence intervals). In contrast, adults with a completely compromised cranial lateral line ('No cLL', in gray, *N*=78) showed vergence less than one-fifth of the time, a highly-significant difference (see text for statistics).

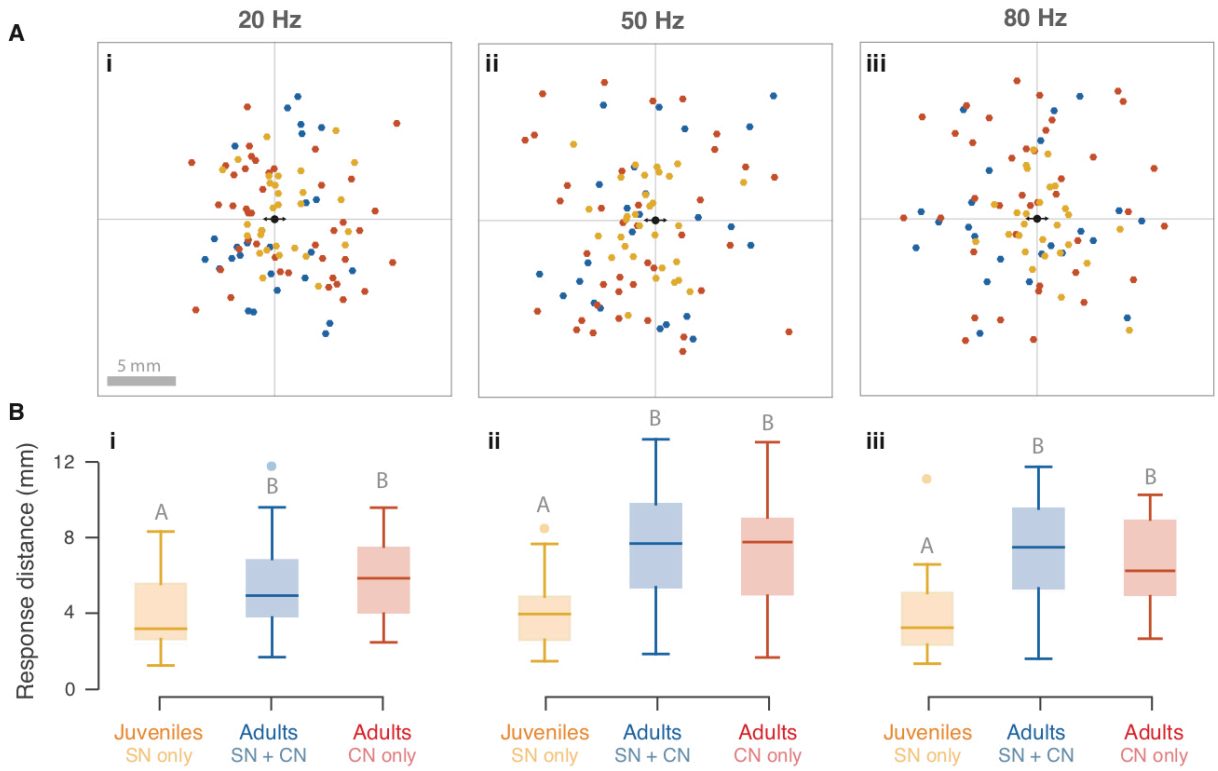

Figure 5: Response distance to the vibrating rod stimulus. Measurements of eye vergence (Fig. 1C–D) were used to identify the response position of fish for stimulus frequencies of (i) 20 Hz, (ii) 50 Hz, and (iii) 80 Hz, arranged in columns. Responses were measured for juveniles (in orange), untreated adults (in blue), and treated adults (in red) where the functioning of the cranial superficial neuromasts were compromised by experimental manipulation. (A) The response position (measured at the center of the head) with respect to the vibrating rod (in center of plot) and the direction of oscillation (parallel to the horizontal axis). (B) The response distance for each group, displayed as boxplots where the filled area extends from the first to third quartiles, with a center line at the median and error flags span the range, and filled circles show outliers. Groups found to be statistically distinct are labeled with different capital letters (see text for statistics).

Discussion

I found that CNs enhance the ability of zebrafish to forage in the dark. This finding was established by behavioral comparisons between juveniles and adults (Fig. 2) and through experimental manipulation (Figs. 3–5). These findings on zebrafish are consistent in a number of respects with previous research on prey localization in the mottled sculpin (Coombs and Conley, 1997a,b; Conley and Coombs, 1998) and other fishes (Ćurcic-Blakĕ and van Netten, 2006; Goulet et al., 2008). Our results support the idea that CNs generally aid in localizing prey, but that their specific function may depend on the size of the predator and its prey.

Canal neuromasts enhance foraging

Adult zebrafish, which have CNs, showed a bite rate to high frequency stimuli ($50 < f < 100$ Hz) that was greater than that of juveniles, which do not have CNs (Fig. 2A). At lower frequencies ($f \leq 50$ Hz), bite rates did not differ between adults and juveniles, which suggests that SNs and CNs mediate foraging equally to prey that operate under this flow regime. Similarly, adults responded to stimuli from a slightly greater distance at low frequency (20 Hz), but at more substantial distances for high frequencies (50 and 80 Hz; Fig. 5). It is conceivable that these differences in behavior are not attributable to the presence of CNs because adult fish could be different in a variety of ways (e.g. an enhanced central nervous system or more opportunity for learning) that yield higher foraging performance when compared to juveniles. This possibility was addressed through our experimental manipulations of adults (Fig. 3). I found that adults with compromised cranial SNs showed the same probability of vergence (Fig. 4) and responded to flow stimuli from an equal distance (Fig. 5) as control adults. Therefore, the CN sensitivity is

sufficient to account for the enhanced behavioral responsiveness of adults.

The results of present experiments share a number of similarities with previous research on the lateral line in fishes larger than zebrafish. Research on prey localization in the mottled sculpin (*Cottus bairdi*) is particularly noteworthy because it offers perhaps the most comprehensive understanding for the role of flow sensing in the behavior of any animal (McHenry and Liao, 2013). In addition, results on the sculpin appear to apply to a variety of fishes, as they have been subsequently replicated in studies on the ruffe (Ćurcic-Blakĕ and van Netten, 2006), and goldfish (Goulet et al., 2008). As I report for zebrafish, the sculpin bites at a vibrating object in the dark after directing its swimming toward this stimulus source (Hoekstra and Janssen, 1985; Coombs and Conley, 1997a). Consistent with our findings, ablating the lateral line in sculpin extinguishes this behavior (Conley and Coombs, 1998), which suggests that flow stimuli are sufficient for prey localization. Remarkably, zebrafish in our study further exhibited eye convergence in the dark when redirecting swimming towards the flow stimuli. Eye vergence is a discrete behavioral response that is likely initiated in response to a threshold of stimulus intensity, which served as a non-conditional response to identify the moment of flow detection in zebrafish to the vibrating rod. In addition, experimental removal of SNs has shown that CNs have been shown to be sufficient to exhibit the behavior in the sculpin (Coombs et al., 2001), much like what I have found for zebrafish (Fig. 5).

The canal neuromasts in zebrafish

The zebrafish lateral line contrasts that of some larger species that may additionally influence how prey are detected. The sculpin, ruff, and goldfish all possess a series of CNs that extend over the length of a body at high density, which forms a visible trunk

lateral line. The central neurophysiological mechanism for this system's ability to localize a food source has yet to be conclusively demonstrated (Ćurcic-Blakĕ and van Netten, 2006; Goulet et al., 2008), but there is strong indication that it is aided by the fact that the trunk spans the body length to an extent that is likely able to detect a stimulus source. In contrast, our results suggest that the trunk lateral line of zebrafish is insufficient for prey localization. When I compromised the cranial neuromasts and left the trunk lateral line intact, the zebrafish would not bite at the rod and ceased to exhibit vergence almost entirely (Fig. 4). The trunk lateral line may not play a large role in foraging in zebrafish because it may not include a series of CNs that run the entire length of the body. Therefore, zebrafish lack a trunk lateral line system that might be able to localize a dipole stimulus.

It has been previously demonstrated that the neuromasts morphology that comprise the lateral-line system plays an important role to flow sensitivity. I found that the canal size and neuromast area in the cranium of 90-dpf zebrafish (mean standard length=17.13, range: 15.20-18.42 mm) in this study were comparable to those reported in previous studies for trunk CNs (Wada et al., 2014). In zebrafish from this study, the canal measurements observed were similar to zebrafish of 15 to 18 mm standard length, and the neuromast area was similar those of 22 to 27 mm to those reported by Wada (2014). As full-grown adults (34 mm standard length) the canal diameter and the neuromasts area have been reported to be twice the size of those measured in this study (Wada et al., 2104). This two-fold increase of CNs morphology may further expand the sensitivity to flows of full-size adults, as they can accommodate more hair cells than that of 90-dpf adults in our study. This potential increase to flow sensitivity resulting from larger CNs in older zebrafish is

predicted to improve foraging responses to perturbations generated by swimming prey.

CHAPTER 3: FORCES DETECTED BY THE RECEPTORS OF THE LATERAL-LINE SYSTEM OF ZEBRAFISH

Introduction

The lateral line of a vast majority of teleost fishes is unique among animals, because they possess two types of receptor, the canal neuromasts (CNs) and the superficial neuromasts (SNs). As described previously (see chapter 2) both receptor types are hair-cell mediated flow receptors that differ in morphology. Residing on the skin, the SNs of the fish as a cluster of hair cells that are deflected by flow through their coupling to an extracellular structure, known as the cupula. A SN is sensitive to the flow velocity of most relevant frequencies because its deflections are created by viscous drag (van Netten and McHenry, 2013). The lateral line of teleost fishes is unique among animals because it also includes a second type of receptor, the canal neuromast (CN). A CN is also a hair-cell mediated flow receptor, but its hemispherical cupula resides within a canal beneath the body's surface. These canals are generally opened to the surface via pores that induce flow through the canal with a difference in pressure. As a consequence, CNs respond to spatial gradients in pressure, such as those generated by an accelerating flow field (Denton and Gray, 1983). Due to the distinct sensitivity of SNs and CNs, the fish lateral line is described as possessing two submodalities of flow sensing (Coombs and Montgomery, 1999) that exhibit contrasting responses to flow stimuli. CNs are considered to be more sensitive to an oscillating flow stimulus (van Netten and McHenry, 2013), and in the results

of the previous study (see Chapter 2) it is clear that CNs allows fish to detect high-frequency flows. It remains unclear what flows CNs and SNs are capable of detecting in zebrafish, which is the purpose of this third chapter.

The role that CNs play in behavior has perplexed biologists since their discovery. It is clear that CNs are not necessary for the lateral-line system to mediate some behaviors. For example, larval fishes generally do not possess CNs, yet their lateral line mediates escape responses to an approaching predator (Stewart et al., 2014; Nair et al., 2017) and rheotaxis (Oteiza et al., 2017). In some lineages, CNs have been secondarily lost (Wark and Peichel, 2010), with no qualitative deficits in behavior. Nonetheless, CNs have been retained among a broad diversity of fishes, which suggests that this submodality offers some functional benefit. Perhaps the most compelling case for the value of CNs is offered by the prey localization behavior in the nocturnal foraging of the mottled sculpin. Hydrodynamic models of the oscillating flow generated by a prey (Kalmijn, 1989) successfully predict the nervous patterns generated by CNs along the length of the body (Coombs and Montgomery, 1999) and experimental ablation of SNs showed no significant effect on this behavior (Coombs et al., 2001). This essential role of the CNs applies to other species of fishes that are similar in size (Ćurčić-Blake and van Netten, 2006; Goulet et al., 2008). This research suggests that the ability to localize a stimulus requires an array of CNs that are distributed along the trunk is comparable in length as the distance to the stimulus (Jannsen, 1997). In addition, the dipole model that predicts the lateral line responses is inviscid and therefore neglects the boundary layer flows that excite SNs. It is therefore unclear how CNs play a role in the foraging behavior of smaller animals and whether SNs might play a larger role in foraging in a different hydrodynamic regime.

Materials and Methods

Nueromast morphology of zebrafish

Photographs from untreated adult (90 dpf) zebrafish collected for chapter 2 experiments were used for morphological measurements of their SN and CN. The images of neuromasts stained with DASPEI were used to provide the basal footprint of neuromasts for biophysical modeling. The linear the dimensions of the bundle of hair cells in cranial SNs and CNs from images of untreated fish were measured to approximate the basal area. The size of this region was assumed to approximately a circular (in SNs) or an elliptical (in CNs) base of the cupula. Basal measurements were performed with Fiji software (version 1.0, ImageJ, Madison, WI, USA). The width of the bony canals at the location of CNs were also measured using Fiji software from the images of the supraorbital CNs, in which the canal was clearly visible. Both the basal area of SNs and CNs and the width of the canal neuromasts were used to predict sensitivity to flows generated by oscillating rod as described below.

Flow visualization of the oscillating rod

The flow field generated by the oscillating rod was measured to understand the stimulus to which the fish responded in our behavioral experiments (see chapter 2). I visualized flow with digital particle image velocimetry (DPIV) using a microscale brightfield approach (Gemmell et al., 2013). I placed the oscillating rod within a rectangular chamber (2 x 4 cm wide and 5 cm tall) constructed of optical glass and illuminated using a 150W fiber optic light (Fisher Scientific, Waltham, MA, USA). The viewing vessel was filled with filtered water and seeded with hallow glass spheres (dia.=120 μm) with a sinking speed that was negligible compared to measured flow velocities. I actuated the rod at various frequencies

between 1 and 100 Hz and recorded flow with high-speed video camera (Photron Fastcam SA3 with a 20mm, Nikon Micro Nikkor lens). The shallow depth-of-field achieved with this arrangement provided a single in-focus slice (~0.2 mm thick) of the moving tracer particles. Depending on the oscillation frequency, the camera recorded images at a rate of 500, 1000, or 2000 frames s^{-1} (with a shutter speed of 263, 333, or 333 μs, respectively) at 1024 x 1024-pixel resolution with a 4.12 mm square field of view. I repeated image collection for the plane in which the rod was oscillating ('in-plane') and the plane normal to the oscillation ('out-of-plane'). Images were processed using the MATLAB-based software PIVlab (Thielicke and Stamhuis, 2014).

The acquisition of particle motion with DPIV posed some special challenges. To avoid interfacial distortion and artifacts, I masked the rod and its mount prior to computing the velocity fields. Due to the high dynamic range of velocity within the image area, I employed a novel approach to the time resolution of the vector fields. A high time resolution was necessary to resolve the vectors very close to the rod, but such a short interval was insufficient for reliable estimation of sub-pixel tracer displacements in the far field. I therefore computed the vector fields for each dataset at several time resolutions, using a small interval for the flow near the rod and a large interval for far-field flows. I additionally employed a multipass algorithm that used an initial 64 x 64 pixel and subsequent 32 x 32-pixel interrogation windows, with a Gaussian subpixel estimator.

Our analysis of the DPIV measurements focused on variation in flow with distanced from the surface of the rod, at the depth of the thickest region of the rod's end. This depth approximated where the fish were found to strike at the rod. Preliminary results showed that the flow velocity oscillated at the frequency of the rod's vibrations with a

peak-to-peak amplitude that I measured by the range of velocity values over time. I additionally found that a streaming current was generated around the vibrating rod, which I measured by the mean value of velocity. The range and mean values at a series of positions away from the surface of rod along were recorded for both the in-plane and out-plane (Fig. 6F–G). The range, R, declined rapidly with distance from the rod. This decline was most rapid within 0.5 mm of the surface of the rod. Beyond that distance, where the animals generally responded, the spatial variation in flow was well-characterized by an exponential function:

$$R = R_0 e^{-l/\lambda_R}, \tag{1}$$

where l is the distance from the surface of the rod, R_0 is the range at a distance of 0.5 mm, and λ_R is the spatial decay constant in the range. The mean velocity, M, showed a similar spatial pattern, though with different parameter values:

$$M = M_0 e^{-l/\lambda_M}, \tag{2}$$

where M_0 is the range at a distance of 0.5 mm, and λ_M is the spatial decay constant in the mean. I used a non-linear least-squares fit ('nlinfit' in MATLAB) of our flow measurements to find parameter values to Eqn. 1 and 2.

Biophysical modeling of neuromasts

I used biophysical modeling to estimate the mechanical sensitivity of neuromasts to flow stimuli. These models formulated predictions based on our measurements of the dimensions of the hair cells within CNs and SNs using the same visualization techniques as were used to verify our experimental treatments (detailed see chapter 2). The biophysical models formulated the frequency-dependent sensitivity of a neuromast as a

transfer function (S) that calculated the deflection of a neuromast's hair cells, per unit flow velocity. Hair cell deflection is the focus of sensitivity because previous work established that the hair cells transduce deflections in proportion to the intensity of a flow stimulus (van Netten and Kroese, 1989; Kroese and van Netten, 1989). The frequency response was characterized by the magnitude of the transfer function ($|S|$) and the phase as its argument ($\arg(S)$) (Lathi, 2009), although our reported results focused only on the response magnitude. In addition to considering the frequency response, I calculated the predicted hair cell deflection in the time domain for the flow stimuli that I measured for our experiments. I modeled the response of CNs first by calculating the acceleration of a flow signal, because CN sensitivity has previously been formulated with respect to acceleration (van Netten and Kroese, 1989).

The sensitivity of a CN depends both on the hydrodynamics of the canal and the dynamics of the neuromast. As a consequence of the viscous flow within the canal generated by pressure differences at its (Denton and Gray, 1983), the canal serves as low-pass mechanical filter like viscous flow through a cylindrical channel (Schlichting, 1979). In this context, the mechanical sensitivity may be defined as the flow velocity in the center of the canal (U_{can}), normalized by the acceleration of freestream flow (A) outside of the channel (van Netten and McHenry, 2013). A numerical solution for the frequency response of the sensitivity for the canal may be calculated by the following equation (van Netten, 2006):

$$S_{\text{can}}(f) = \frac{U_{\text{can}}}{A} = \begin{cases} H_{\text{can}}(f), & \text{for } f < f_{\text{s}} \\ \text{conj}\left(H_{\text{can}}(f)\right), & \text{for } f \geq f_{\text{s}}, \end{cases} \tag{3}$$

where

$$H_{\mathrm{can}}(f) = \left[2\pi f_{\mathrm{can}} \left(\frac{f}{f_{\mathrm{can}}} i\right)\right]^{-1}, \tag{4}$$

f is the stimulus frequency, f_s is the Nyquist frequency (i.e. half the sampling rate) and f_{can} is the cut-off frequency of the canal. The cut-off frequency is given by the following relationship:

$$f_{\mathrm{can}} = \frac{\mu_{\mathrm{can}}}{\rho R^2}, \tag{5}$$

where μ_{can} and ρ are respectively the dynamic viscosity (μ_{can} = 5.1 mPa s, (van Netten and Kroese, 1987; Kroese and van Netten, 1989) and density (ρ=1000 kg m^{-3}) of fluid in the canal and R is the canal radius.

The sensitivity of the CN additionally depends on the fluid-structure interaction between the flow within the canal and the neuromast. The cupula of the canal neuromast is modeled as a rigid hemisphere that is elastically-coupled to the wall of the canal via hair cells. Deflections of the hair cells (D) are thereby driven by fluid forces acting on the cupula. This biophysical model has been verified by deflection measurements using laser interferometry (van Netten and Kroese, 1987; van Netten and Kroes, 1989). The frequency response may be calculated numerically with the following relationship (van Netten, 2006)

$$S_{\mathrm{cup}}(f) = \frac{D}{U_{\mathrm{can}}} = \begin{cases} H_{\mathrm{cup}}(f), & \text{for } f < f_{\mathrm{s}} \\ \mathrm{conj}\left(H_{\mathrm{cup}}(f)\right), & \text{for } f \geq f_{\mathrm{s}}, \end{cases} \tag{6}$$

where:

$$H_{\mathrm{cup}} = \frac{\frac{1}{2\pi f_{\mathrm{t}}} + \frac{0.5\sqrt{2}(i-1)\sqrt{f}}{2\pi i}\left(\frac{1}{f_{\mathrm{t}}}\right)^{\frac{3}{2}} - \left(\frac{1}{f_{\mathrm{t}}}\right)^2 \frac{1}{6\pi i}}{p_{\mathrm{c}} + \frac{f}{f_{\mathrm{t}}} i + \frac{\sqrt{2}}{2}(i-1)\left(\frac{f}{f_{\mathrm{t}}}\right)^{\frac{3}{2}} - \frac{1}{3}\left(\frac{f}{f_{\mathrm{t}}}\right)^2}, \tag{7}$$

f_t is the transition frequency, and p_c is a dimensionless physical constant for the cupula. These parameters are defined as follows:

$$p_c = \frac{nk_{CN}a\rho}{6\pi\mu_{can}^2}, \tag{8}$$

$$f_t = \frac{\mu_{can}}{2\pi\rho a^2}, \tag{9}$$

where a is the radius of the cupula, n is the number of hair cells, k_{CN} is the sliding stiffness of a single hair cell (k_{CN} = 0.13 mN m^{-1}) (van Netten and Kroese, 1987; van Netten and Kroes, 1989). I approximated a as half the mean value of the width (W, i.e. linear dimension crosswise with respect its canal) and length (L, i.e. linear dimension along the canal). The number of hair cells was estimated from measurements length, according to the following relationship, established previously (Webb and Shirey, 2003):

$$n = (0.421\ \mu m^{-1})L + 15.426, \tag{10}$$

where L is entered with units of microns. The sensitivity of the hair cells to the acceleration of flow was calculated as the product of canal (Eqn. 3) and neuromast (Eqn. 11) sensitivity:

$$S_{CN} = S_{cup}S_{can}. \tag{11}$$

I similarly employed a biophysical model of the SNs to estimate their sensitivity. The superficial neuromasts reside within the boundary layer of flow over the surface of the body. The SN cupula is elongated and composed of highly compliant material (McHenry and van Netten, 2007), which bends in flow (Liao, 2010). The mechanical filtering of this type of neuromast depends on the frequency-dependent hydrodynamics of

the boundary layer and the fluid-structure interaction between this flow and the beam dynamics of the SN cupula. The combined influence of these mechanics generates a sensitivity of hair cell deflection to a freestream velocity stimulus (U_∞), given by the following relationship (McHenry et al., 2008; Yoshizawa et al., 2014):

$$S_{\mathrm{SN}} = \frac{D_{\mathrm{SN}}}{U_\infty} = K_{\mathrm{low}} K_{\mathrm{comp}} \frac{\sqrt{2if}}{1 + \left(\frac{K_{\mathrm{low}}}{K_{\mathrm{high}}}\right)\sqrt{2if}} \tag{12}$$

where the compliance parameter (K_{comp}), and low-frequency (K_{low}) and high-frequency (K_{high}) parameters are given as follows:

$$K_{\mathrm{comp}} = \frac{2.37\sqrt{\rho}}{n k_{\mathrm{SN}}}, \tag{13}$$

$$K_{\mathrm{low}} = h^2\sqrt{\mu_{\mathrm{SN}}}, \tag{14}$$

and

$$K_{\mathrm{high}} = \frac{1}{4} w^2 \sqrt{E}, \tag{15}$$

where k_{SN} is the stiffness of a hair cell (k_{SN} = 1 mN m^{-1}), h is the cupula height, w is the width of the cupula, and E is the Young's modulus of the cupula. I relied on previous measurements of cupula height (Van Trump and McHenry, 2008) and treated it as a fixed parameter (h = 50 μm) in our comparisons.

Results

I measured the flow field generated by the vibrating rod used in our experiments with DPIV. This included measurements along a plane parallel to the direction of vibration

(i.e. 'in-plane') and a plane perpendicular (i.e. 'out-plane', Fig. 1A–C). In both directions, the flow velocity oscillated at the frequency of the rod's vibrations (Fig. 1D–E). Streaming flow toward or away from the rod was apparent by non-zero values for the mean velocity. The range and mean values were found for a series of positions away from the surface of the rod along both the in-plane and out-plane (Fig. 1F–G). Both metrics decreased exponentially with distance, as indicated by strong agreement of functions for exponential decay (Eqns. 1 and 2, Table 1, $r^2>0.90$) for the range and mean values for velocity.

Our measurements of flow were interpreted as a stimulus for the lateral line system through the use of biophysical modeling. These models considered the measured dimensions of each neuromast (summarized in Table 2) to model the hair cell deflection for both CNs (Eqn. 11) and SNs (Eqn. 12). Both types of neuromast were predicted to function as high-pass filters of flow velocity (Fig. 2A) for the range of stimulus frequencies that I considered (0.1 Hz$<f<$1000 Hz). At the lower end of this frequency range, SNs proved to be more sensitive than CNs. For example, using the median morphometrics (Table 2), the sensitivity of SNs ($\tilde{x}$=0.72 nm/mm s^{-1}) was nearly 4-times more sensitive than CNs ($\tilde{x}$=0.17 nm/mm s^{-1}) at 1 Hz. In contrast, the two types of neuromast showed similar sensitivity to a 10 Hz stimulus (SN: $\tilde{x}$=1.83 nm/mm s^{-1}, CN: $\tilde{x}$=1.81 nm/mm s^{-1}). The most notable difference was apparent at higher frequencies, where CNs were more sensitive than SNs. For example, CN-sensitivity ($\tilde{x}$=20.8 nm/mm s^{-1}) was more than an order of magnitude greater than that of SNs ($\tilde{x}$=1.45 nm/mm s^{-1}) for a 100 Hz stimulus. Therefore, CNs present some advantages to sensing flow, but only at relatively high frequencies.

The frequency responses of neuromasts were used to interpret behavioral responses to flow. As detailed in Chapter 2, the adults bit at the vibrating rod more often than juveniles at relatively high stimulus frequencies, particularly at $50<f<100$ Hz (Fig. 2A–B). Predictions of sensitivity to flow velocity were formulated using the median frequency responses (Fig. 3) for the frequencies used in behavioral experiments. This revealed a similar pattern in sensitivity (Fig. 3C), as observed in adult behavior. At low frequencies ($2<f<10$ Hz), adults and juveniles were indistinguishable in bite rate and the two types of neuromast showed comparable responses ($\tilde{x}$=1.80 nm/mm s^{-1} for CNs, $\tilde{x}$=1.83 nm/mm s^{-1} for SNs, N=64). At medium frequencies ($10<f<50$ Hz), where adults showed a significantly higher bite rate, CNs were predicted to be more than 4-times more sensitive ($\tilde{x}$=9.87 nm/mm s^{-1} N=64) than SNs ($\tilde{x}$=2.16 nm/mm s^{-1}, N=64). Similarly, CNs ($\tilde{x}$=20.8 nm/mm s^{-1}, N=64) were more than an order of magnitude more sensitive than SNs ($\tilde{x}$=1.62 nm/mm s^{-1}, N=64) to high-frequency ($50<f<100$ Hz) stimuli, where bite rate was higher in adults. Despite these similarities between behavior and our modeling, it is noteworthy that higher frequencies yield more than a 10-fold sensitivity difference, whereas bite rate is different only by a factor of three.

Using our measurements of flow velocity (Fig. 1) and biophysical modeling (Fig. 2), I estimated responses of neuromasts at different positions in the flow field. Here, the responses of neuromasts were formulated as the predicted deflection of hair cells within SNs and CNs, determined by the product of flow velocity and neuromast sensitivity. This calculation showed that hair cell deflection exhibited a monotonic decrease with distance from the vibrating rod (Fig. 3B), due to the spatial decay in flow (Fig. 1F–G, 3A). I calculated hair cell deflection at the positions in the flow fields where juveniles and adults

responded with eye vergence. At 20 Hz, adults responded from a 60% greater distance then juveniles (Fig. 4Ai–Bi). CNs showed a comparable response at the adult distance ($\tilde{x}$=0.18 nm, N=68) than SNs at the juvenile distance ($\tilde{x}$=0.15 nm, N=30). This supports the idea that enhanced CN sensitivity is sufficient to enable adults to respond at greater distance. However, the responses at high frequencies offer a slightly more complex interpretation. CNs showed about a 2-fold greater response the response position of adults (50 Hz: $\tilde{x}$=0.26 nm, N=62; 80 Hz: $\tilde{x}$=0.16 nm, N=23) than the response of SNs at the position of juveniles (50 Hz: $\tilde{x}$=0.11 nm, N=62; 80 Hz: $\tilde{x}$=0.06 nm, N=23). This would appear to suggest that adults could respond from a greater distance than I observed. Nonetheless, the results at higher frequencies is consistent with the notion that CNs allow adult fish to sense an enticing stimulus from greater distance than would be possible from SNs alone.

Table 1: Spatial decay in flow velocity

	In-plane		Out-plane	
	u	w	v	w
20 Hz				
M_0	0.002	0.295	0.100	0.068
λ_M	18.3	37.0	6.71	1.01
R_0	1.84	0.815	0.982	0.877
λ_R	0.555	0.933	0.155	0.280
50 Hz				
M_0	0.147	0.364	0.174	0.195
λ_M	0.960	20.9	3.74	9.06
R_0	4.14	1.53	1.28	0.386
λ_R	0.454	0.700	0.438	1.55
80 Hz				
M_0	0.185	0.371	0.0117	0.170
λ_M	1.58	3.07	37.7	4.90
R_0	5.69	2.05	2.05	0.462
λ_R	0.472	0.673	0.339	0.743

M_0, Initial value of mean; λ_M , Spatial decay in mean;
R_0 Initial value of range; λ_R, Spatial decay of range.

Table 2: Morphometrics of the lateral line

	Median	Minimum	Maximum	N
SN neuromast				
a (µm)	8.2	6.0	10.6	15
Infraorbital CN neuromast				
W (µm)	34.9	23.5	47.9	16
L (µm)	54.5	32.1	78.4	16
Supraorbital CN neuromast				
W (µm)	44.4	37.6	61.7	16
L (µm)	77.6	62.1	90.1	15
Infraorbital CN canal				
R (µm)	36.2	25.4	45.1	15
Supraorbital CN canal				
R (µm)	50.1	38.5	62.8	15

a, SN Cupula radius; *W*, CN cupula width; *L*, CN cupula length; *R*, Canal radius.

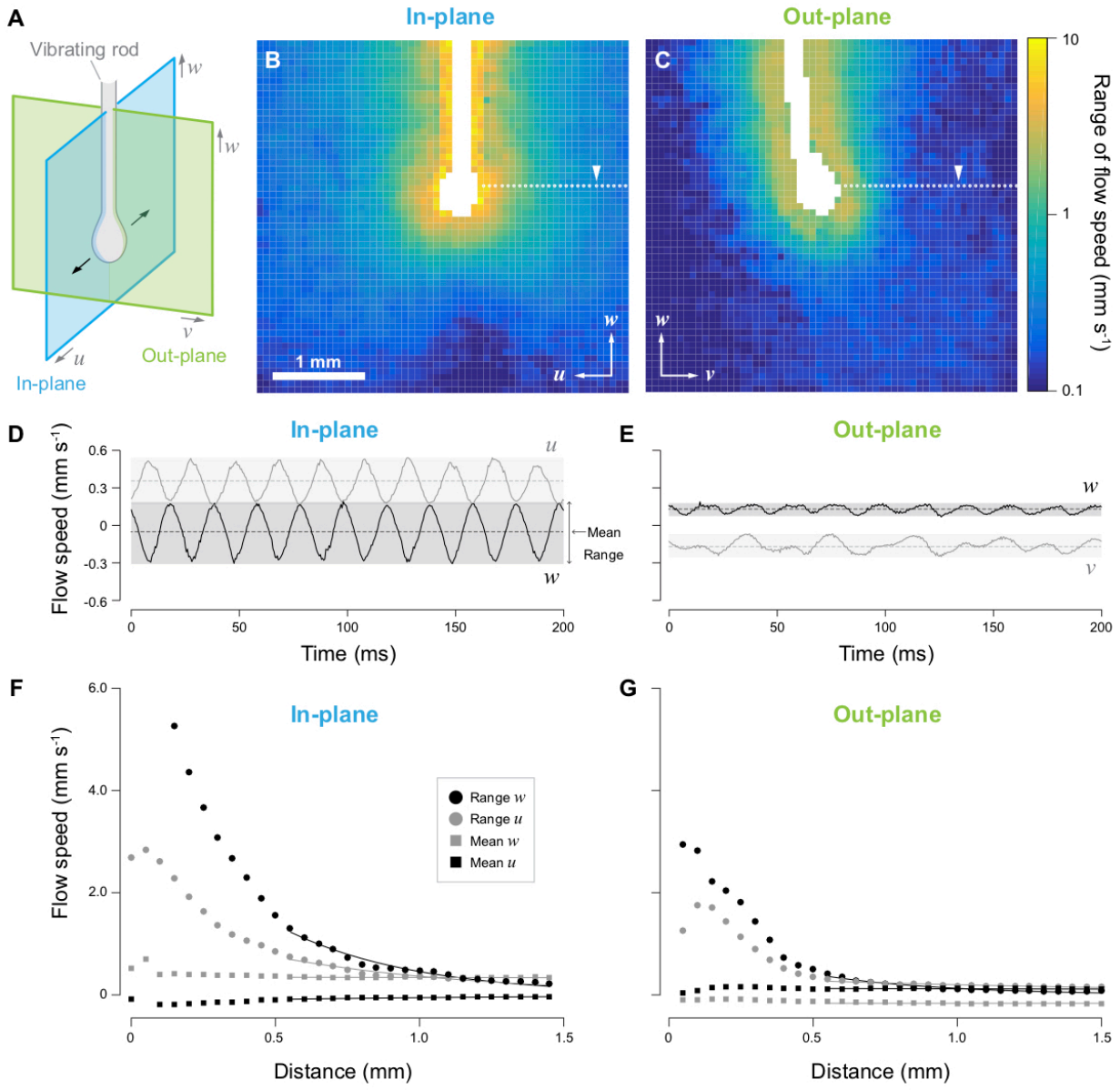

Figure 1: Flow visualization of stimulus created by oscillating rod. (A) The displacement of particles was recorded for planes parallel ('In-plane') and perpendicular ('Out-plane') to the direction of vibration. The flow speed decreased rapidly with distance from the rod for both the (B) in-plane and (C) out-plane, as indicated by the three orders-of-magnitude range of variation spanned in the flow field. Flow velocity at a particular position (white arrowhead in B and C) show the oscillations in velocity both (D) in-plane and (D) out-plane. The mean values (dashed lines) and range (gray areas) indicate the respective unidirectional and oscillatory components of flow velocity. The attenuation in both the mean and range with distance were characterized by a non-linear least-squares curve-fit of a decay function for both (B) in-plane and (C) out plane flows.

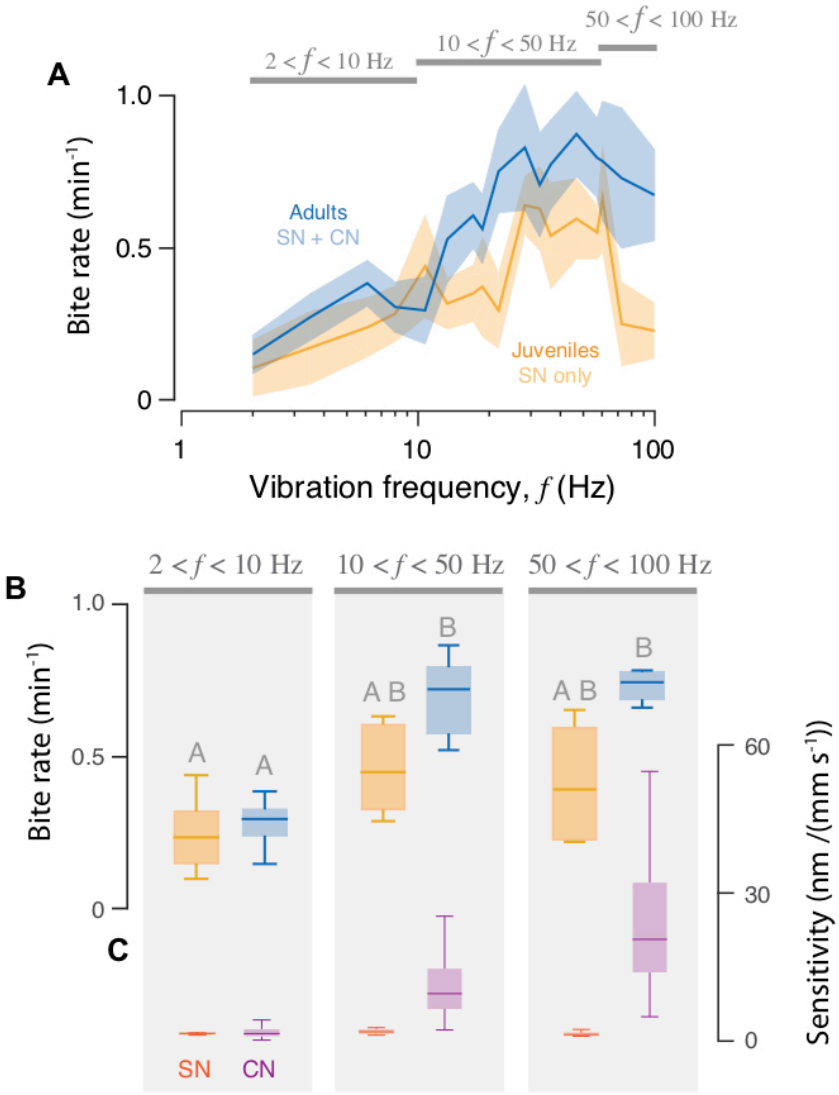

Figure 2: The behavioral frequency response and sensitivity to a vibrating rod. (A) The bite rate is the frequency by which an individual struck at the vibrating rod placed in the center of a petri-dish (Fig. 1A). These experiments were performed with 14 groups of 5 adult (in blue) and juvenile (in orange) fish ($N = 7$; Data from Chapter 2). (B) I performed statistical comparisons in bite rate between adults (in blue) and juveniles (in orange) for groups of frequencies. I found significant effects of both age and vibration frequency, with post-hoc groups denoted by capital letters (see text for statistics). (C) Similar trends were predicted for the sensitivity of CNs and SNs, as predicted by our bio- physical modeling (Fig. 7). The filled area of each boxplot extends from the first to third quartiles, with a center line at the median value and error flags that span the range.

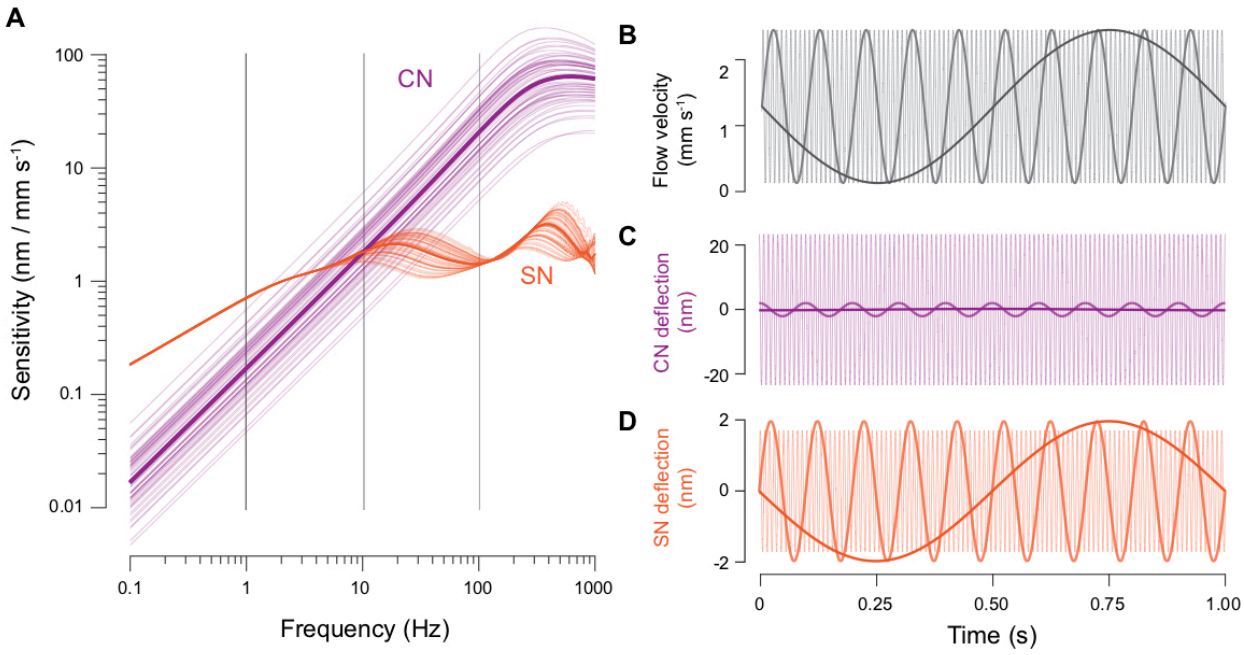

Figure 3: Biophysical models of cranial neuromasts, based on morphometric measurements. (A) The frequency response of CNs (in violet, Eqns. 3 and 11) and SNs (in red, Eqns. 12), with light curves showing predictions for an individual neuromast and the heavy curve indicating the median value. (B) Simulated flow velocities are plotted in the time domain at 1, 10, and 100 Hz. For those stimuli, the hair cell deflections predicted for the median (C) CN and (D) SN are shown.

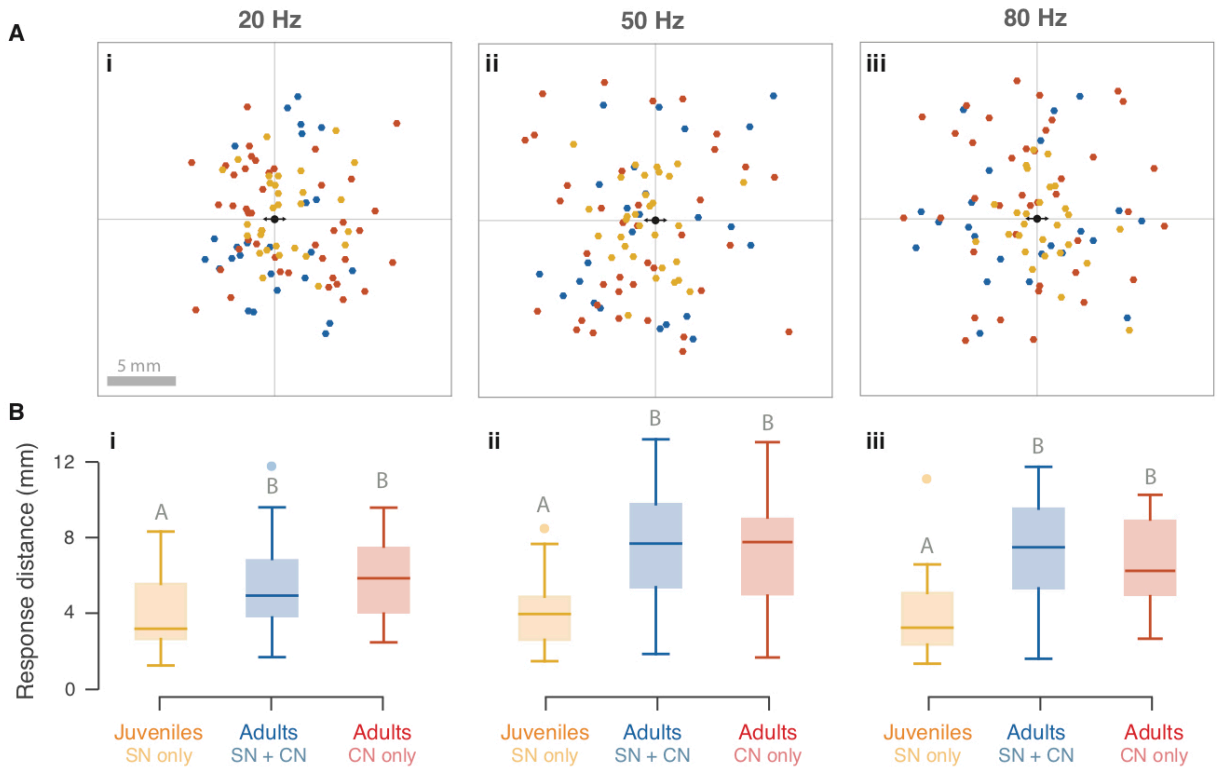

Figure 4: Response distance to the vibrating rod stimulus (From Chapter 2). Measurements of eye vergence (Fig. 1C–D) were used to identify the response position of fish for stimulus frequencies of (i) 20 Hz, (ii) 50 Hz, and (iii) 80 Hz, arranged in columns. Responses were measured for juveniles (in orange), untreated adults (in blue), and treated adults (in red) where the functioning of the cranial superficial neuromasts were compromised by experimental manipulation. (A) The response position (measured at the center of the head) with respect to the vibrating rod (in center of plot) and the direction of oscillation (parallel to the horizontal axis). (B) The response distance for each group, displayed as boxplots where the filled area extends from the first to third quartiles, with a center line at the median and error flags span the range, and filled circles show outliers. Groups found to be statistically distinct are labeled with different capital letters (see text for statistics).

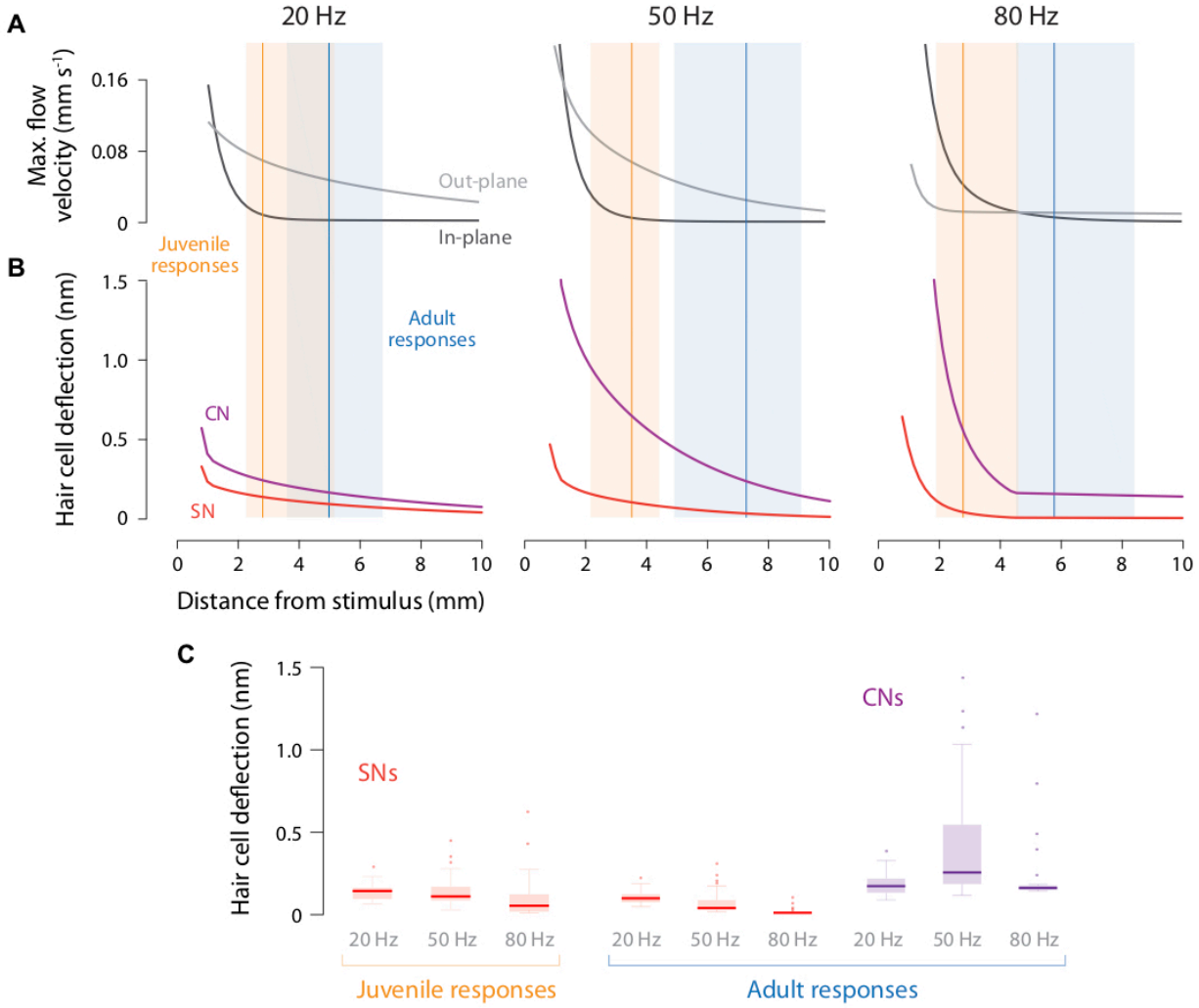

Figure 5: Modeled responses of SNs and CNs in behavioral experiments.
(A) Measurements of flow in the in-plane (in black) and out-plane (in gray, Fig. 1A) for stimuli of 20, 50, and 80 Hz. From these flow measurements, (B) I used biophysical models (Fig. 3) to predict the deflection of hair cells for the median CN (in purple) and SN (in red). The median (vertical lines) and range (colored rectangles) of measured response distance for juveniles (in orange) and adults (in blue) are shown. (C) Predictions of hair cell deflection were formulated from our flow measurements (Fig. 1), measurements of response distance (Fig. 4), and morphometrics of neuromasts. These predictions were determined for SNs (in red) and CNs (in purple) in juveniles (in orange) and adults (in blue). In each boxplot, the filled area extends from the first to third quartiles, with a center line at the median and error flags span the range, and filled circles showoutliers.

Discussion

I measured the flow field generated by our artificial stimulus (Fig. 1) and modeled the frequency responses of CNs and SNs (Fig. 2) to estimate the stimuli detected by the lateral line from behavioral experiments from Chapter 2. These findings on zebrafish are consistent in a number of respects with previous research on prey localization in the mottled sculpin (Coombs and Conley, 1997a,b; Conley and Coombs, 1998) and other fishes (Ćurcic-Blakě and van Netten, 2006; Goulet et al., 2008) that are about ten times the length of zebrafish adults. However, there are sufficient differences in hydrodynamic scale and lateral line morphology between zebrafish and these larger species to suggest that fishes of different size sense prey in a manner that is fundamentally distinct.

I developed a prey mimic to generate a controlled flow stimulus that elicited feeding behavior. Fish would bite at our vibrating rod with a suction-feeding strike that is similar to what has been previously observed for zebrafish as they forage on *Artemia* (Carrillo and McHenry, 2016; McElligott and O'Malley, 2005). As when foraging on live prey, zebrafish exhibited eye vergence prior to the approach toward the prey mimic (Fig. 1B–D). Vergence is an unconditioned behavioral response to prey that presumably enhances stereopsis but occurs even when foraging in the dark (CITES). Our measurements of vergence lend further support to the notion that our vibrating rod served as an effective prey mimic while providing the opportunity to use the response distance (Fig. 5) as a measure of behavioral sensitivity.

Foraging behavior depends on neuromast sensitivity

I found a number of ways that the foraging behavior of zebrafish conforms to the predictions of the biophysical models of the neuromasts. Adult zebrafish, which have CNs, showed a bite rate to high frequency stimuli ($50<f<100$ Hz) that was greater than that of juveniles, which do not have CNs. Similarly, CNs are predicted to be substantially more sensitive than SNs for the same

frequencies (Figs. 2B, 3). Furthermore, CNs are only slightly more sensitive than SNs at 20 Hz, but are more superior at 50 and 80 Hz. Similarly, adults responded from nearly twice the distance at 20 Hz, but at more substantial distances for 50 and 80 Hz (Fig. 4). Thus, the CN sensitivity is sufficient to account for the enhanced behavioral responsiveness of adults (Figs. 2, 4)

There were noteworthy discrepancies between the predictions of our biophysical modeling and behavioral measurements. The models predict a greater magnitude of differences in neuromast sensitivity than is shown in behavior. For example, CNs are predicted to be over 10 times as sensitive as SNs to relatively high-frequency stimuli (Fig. 2C), yet adults showed only a 2-fold increase to bite rate than juveniles (Fig. 2B). Similarly, CNs are 15-times more sensitive to a 50 Hz stimulus than are SNs (Fig. 2), but response distance was greater in adults by only a factor of two (Fig. 5). These discrepancies may partially be explained by the nature of the flow field generated by the vibrating rod. Flow velocity showed a rapid attenuation with distance (Fig. 8A). This non-linear relationship requires a disproportionate increase in sensitivity to achieve proportional changes in response distance. If bite rate similarly reflects the probability that a forager moved within this radius around the rod where it may be detected, then it too would be expected to require disproportionate increases in sensitivity for proportional changes in bite rate.

Even when taking the non-linearity of the flow field into account, behavior does not perfectly match our expectations from the model. I used the predicted frequency responses of the neuromasts (Fig. 2A) to estimate the signals that they detect, as a function of distance from the rod (Fig. 5). According to this formulation, the adults that possess CNs do respond from greater distance (Fig. 5B), but still experience up to 15 times greater hair cell deflections than in the SNs at the distance of responses by juveniles. This suggests that adults could have responded from an even greater distance than what I observed.

These comparisons of behavior to model predictions neglect the role played by the animal's nervous system. Eye vergence is a discrete behavioral response that is likely initiated in

response to a threshold of stimulus intensity. At the level of the neuromasts, this intensity is transduced by the deflection of the hair cells (van Netten et al., 2003), which demonstrates the value of biophysical models that focus on deflection. However, the nervous system presents a series of opportunities to raise or lower the threshold stimulus that elicits a motor response. At the neuromasts level, threshold sensitivity is thought to be determined by the ratio of hair cell deflection to the Brownian gating spring noise that is inherent to mechanotransduction (van Netten et al., 2003). This noise is inversely proportional to the square root of the number of hair cells. For the adult zebrafish presently considered, the CNs possessed around 44 hair cells (Webb and Shirey, 2003), which is approximately 3.7 times the number of hair cells as the SNs (Van Trump and McHenry, 2008). This suggests that CN have about half the threshold sensitivity of SNs, at a level of ~1 nm (van Netten, 2006). However, this consideration neglects the role of integration in the peripheral nervous system. For example, trunk afferent neurons in zebrafish branch to the hair cells of multiple SNs (Liao, 2010). This raises the possibility that the threshold sensitivity could be improved through the integration of signals across neuromasts at the level of the periphery. Integration could further occur at higher levels of the nervous system to lower the sensory threshold. In support of this idea, I found that almost all behavioral responses were elicited by hair cells deflections of less than 1 nm (Fig. 2C), the threshold predicted for a single CN. In addition, it appears likely that the foraging behavior that I presently considered operates close to the physiological limits of lateral line sensitivity.

REFERENCES

Arkett, S. A., Mackie, G. O. and Meech, R. W. (1988). Hair cell mechanoreception in the jellyfish *Aglantha Digitale*. *J. Exp. Biol.* 135, 329–342. Batchelor, G. K. (1967). *An Introduction to Fluid Dynamics*. New York: Cambridge University Press.

Atema, J. (1971) Structure and functions of the sense of taste in the catfish (*Ictalurus natalis*) *Brain Behav. Evol.* 4: 273-294

Batchelor, G. K. (1967). *An Introduction to Fluid Dynamics*. New York: Cambridge University Press.

Bianco, I. H., Kampff, A. R. and Engert, F. (2011). Prey capture behavior evoked by simple visual stimuli in larval zebrafish. *Front. Sys. Neuros.* 5, 101.

Blaxter, J. H. S. and Fuiman, L. H. (1989). Function of the free neuromasts of marine teleost larvae, In The Mechanosensory Lateral Line: Neurobiology and Evolution (eds. S. Coombs, P. Görner, and H. Münz), pp. 481–499. New York, NY: Springer-Verlag

Bone, Q. and Ryan, K. P. (1978). Cupular sense organs in Ciona (Tunicata: Ascidiacea). *J. Zool.* 186, 417–429.

Borla, M. A., Palecek, B., Budick, S., and O'malley, D. M. (2002). Prey capture by larval zebrafish: evidence for fine axial motor control. *Brain Behav. Evol.*, 60: 207–229.

Brown, L. (1981). Patterns of female choice in mottled sculpins (Cottidae, teleostei). *Ani. Behav.* 29, 375–382.

Braubach, O. R., Wood, H. D., Gadbois, S., Fine, A., and Croll, R. P. (2009). Olfactory conditioning in the zebrafish (Danio rerio). *Behav. Brain Res.*, 198: 190–198

Budelmann, B. U. and Bleckmann, H. (1988). A lateral line analogue in cephalopods: water waves generate microphonic potentials in the epidermal headlines of *Sepia* and *Lolliguncula*. *J. Comp. Physiol. A* 164, 1–5.

Budick, S. A., and O'Malley, D. M. (2000). Locomotor repertoire of the larval zebrafish: swimming, turning and prey capture. *J. Exp. Biol.*, 203: 2565–2579

Carrillo, A. and McHenry, M. J. (2016). Zebrafish learn to forage in the dark. *J. Exp. Biol.* 219, 582–589.

China, V., and Holzman, R. (2014). Hydrodynaic starvation in first-feeding larval fishes. *Proc. Nat. Acad. Sci.*, 111: 8083-8088.

Cobb, J. L. S. and Moore, A. (1986). Comparative studies on receptor structure in the brittlestar, *Ophiura ophiura*. *J. Neurocyt.* 15, 97–108.

Conley, R. and Coombs, S. (1998). Dipole source localization by mottled sculpin. III. Orienation after site-specific, unilateral denervation of the lateral line system. *J. Comp. Physiol.* A 183, 335–344.

Coombs, S., Braun, C. and Donovan, B. (2001). The orienting response of Lake Michigan mottled sculpin is mediated by canal neuromasts. *J. Exp. Biol.* 204, 337–348.

Coombs, S. and Conley, R. (1997a). Dipole source localization by mottled sculpin. I. Approach strategies. *J. Comp. Physiol.* 180, 387–399.

Coombs, S. and Conley, R. (1997b). Dipole source localization by the mottled sculpin. II. The role of lateral line excitation patterns. *J. Comp. Physiol. A* 180, 401–415.

Coombs, S. and Janssen, J. (1990). Behavioral and neurophysiological assessment of lateral line sensitivity in the mottled sculpin, *Cottus bairdi*. *J. Comp. Physiol. A* 167, 557–567.

Coombs, S. and Montgomery, J. C. (1999). The Enigmatic Lateral Line System. In Comparative Hearing: Fish and Amphibians (eds. R. R. Fay and A. N. Popper), pp. 319–362. New York, NY: Springer New York.

Colwill, R. M., Raymond, M. P., Ferreira, L., and Escudero, H. (2005). Visual discrimination learning in zebrafish (Danio rerio). *Behav. Proc.*, 70: 19–31

C´urˇci´c-Blake, B. and van Netten, S. M. (2006). Source location encoding in the fish lateral line canal. *J. Exp. Biol.* 209, 1548–1559.

Dempsey, C. H. (1978). Chemical Stimuli as a factor in feeding and intraspecific behaviour of Herring Larvae. *J. Mar. Biol. Ass. Uni. King.* 58: 739-747.

Denton, E. J. and Gray, J. (1983). Mechanical factors in the excitation of clupeid lateral lines. *Proc. R. Soc. B* 218, 1–26.

Dijkgraaf, S. (1963). The functioning and significance of lateral-line organs. *Biol Rev Cambridge Phil Soc* 38, 51–105.

Fields, D. M. and Weissburg, M. J. (2004). Rapid firing rates from mechanosensory neurons in copepod antennules. *J. Comp. Physiol. A* 190, 877–882.

Fuiman, L. A., Smith, M. E., and Malley, V. N. (1999). Ontogeny of routine swimming speed and startle responses in red drum, with a comparison of responses to acoustic and visual stimuli. *J. Fish. Biol.* 55: 215–226.

Gahtan, E., and O'Malley, D. M. (2003). Visually guided injection of identified reticulospinal neurons in zebrafish: a survey of spinal arborization patterns. *J. Comp. Neuro.,* 459: 186–200

Gahtan, E., Tanger, P., and Baier, H. (2005). Visual prey capture in larval zebrafish is controlled by identified reticulospinal neurons downstream of the tectum. *J. Comp. Neuro.,* 40: 9294–9303.

Gemmell, B. J., Adhikari, D. and Longmire, E. K. (2013). Volumetric quantification of fluid flow reveals fish's use of hydrodynamic stealth to capture evasive prey. *J. Roy. Soc. Interface 11*.

Goulet, J., Engelmann, J., Chagnaud, B. P., Franosch, J. M. P., Suttner, M. D. and Van Hemmen, J. L. (2008). Object localization through the lateral line system of fish: Theory and experiment. *J. Comp. Physiol. A* 194, 1–17.

Harris, J. A., Cheng, A. G., Cunningham, L. L., MacDonald, G., Raible, D. W. and Rubel, E. W. (2003). Neomycin-Induced Hair Cell Death and Rapid Regeneration in the Lateral Line of Zebrafish (*Danio rerio*). *J Assoc. Res. Otolaryn.* 4, 219–234.

Hoekstra, D. and Janssen, J. (1985). Non-visual feeding behavior of the mottled sculpin, *Cottus bairdi,* in Lake Michigan. *Environ. Biol. Fishes* 12, 111–117.

Holzman, R., Day, S. W., Mehta, R. S., and Wainwright, P. C. (2008). Jaw protrusion enhances forces exerted on prey by suction feeding fishes. *J. R. Soc. Interface* 5: 1445–1457

Jannsen, J. (1997). Comparison of response distance to prey via the lateral line in the ruffe and yellow perch. *J. Fish Biol*. 51, 1–10.

Kalmijn, A. J. (1988). Hydrodynamic and Acoustic Field Detection. In Sensory Biology of Aquatic Animals (eds. J. Atema, R. Fay, A. N. Popper and W. N. Tavolga), pp. 83–130.

Kalmijn, A. J. (1989). Functional evolution of lateral line and inner ear sensory systems. In Mechanosensory Lateral Line Neurobiol. Evol. (eds. S. Coombs, P. Go¨rner and H. Mu¨nz), pp. 187–215.

Kroese, A. B. A. and van Netten, S. M. (1989). Sensory Transduction in Lateral Line Hair cells. In The Mechanosensory Lateral Line (eds. S. Coombs, P. Go¨rner and H. Mu¨nz), pp. 265– 284. New York, NY: Springer New York.

Lathi, B. P. (2009). In Signal processing and linear systems. Carmichael, CA: Berkely Cambridge Press.

Lenz, P. H. and Yen, J. (1993). Distal setal mechanoreceptors of the first antennae of marine copepods. *Bull. Mar. Sci.* 53.

Li, J., Mack, J. A., Souren, M., Yaksi, E., Higashijima, S. I., Mione, M., et al. (2005). Early development of functional spatial maps in the zebrafish olfactory bulb. *J. Comp. Neuro.,* 25: 5784–5795

Liao, J. C. (2010). Organization and physiology of posterior lateral line afferent neurons in larval zebrafish. *Biol. Ltrs* 6, 402–405.

Margulies, D. (1989). Size-specific vulnerability to predation and sensory system development of white seabass, *Atractoscion nobilis*, larvae. *Fish. Bull.*, 87: 537-552

McElligott, M. B. and O'Malley, D. M. (2005). Prey tracking by larval zebrafish: axial kinematics and visual control. *Brain Behav Evol* 66, 177–196.

McHenry, M. J. and Liao, J. C. (2013). The Hydrodynamics of Flow Stimuli. In Springer Handbook of Auditory Research 48: The Lateral Line. (eds. S. Coombs, H. Bleckmann, R. R. Fay and P. A. N), pp. 1–26. New York, NY: Springer New York.

McHenry, M. J., Strother, J. A. and van Netten, S. M. (2008). Mechanical filtering by the boundary layer and fluid–structure interaction in the superficial neuromast of the fish lateral line system. *J. Comp. Physiol. A* 194, 795.

McHenry, M. J. and van Netten, S. M. (2007). The flexural stiffness of superficial neuromasts in the zebrafish (*Danio rerio*) lateral line. *J. Exp. Biol*. 210, 4244–4253.

Muki, Y., Yoshikawa, H., and Kobayashi H. (1994). The relationship between the length of the cupulae of free neuromasts and feeding ability in larvae of the willow shiner *Ganthopogon elonatus caerulescens* (Teleostei, Cyprinidae). *J. Exp. Biol.*, 197: 399-403

Muto A., and Kawakami, K. (2013). Prey capture in zebrafish larvae serves as a model to study cognitive functions. *Front. Neur. Circ.* 110: 1–5

Nair, A., Changsing, K., Stewart, W. J. and McHenry, M. J. (2017). Fish prey change strategy with the direction of a threat. *Proc. Royal Soc. B*: Biological Sciences 284.

O'Malley, D. M., Sankrithi, N. S., Borla, M. A., Parker, S., Banden, S., Gahtan, E., and Detrich, H. W. (2004). Optical physiology and locomotor behaviors of wild-type and nacre zebrafish. *Meth. Cell Biol.*, 76: 261–284

Oteiza, P., Odstrcil, I., Lauder, G., Portugues, R. and Engert, F. (2017). A novel mechanism for mechanosensory-based rheotaxis in larval zebrafish. *Nature* 547, 445–448.

Patterson, B. W., Abraham, A. O., MacIver, M. A. and McLean, D. L. (2013). Visually guided gradation of prey capture movements in larval zebrafish. *J. Exp. Biol.* 216, 3071–3083.

Rapo, M. A., Jiang, H. and Grosenbaugh, M. A. (2009). Using computational fluid dynamics to calculate the stimulus to the lateral line of a fish in still water. *J. Exp. Biol.* 212, 494–1505.

Sane, S. P. and McHenry, M. J. (2009). The biomechanics of sensory organs. *Integ. and Comp. Biol.* 49, i8–i23.

Scharrer, E. (1932). Experiments on the function of the lateral-line organs in the larvae of *Amblystoma punctatum. J. Exp. Zool.* 61, 109–114.

Schlichting, H. (1979). In Boundary–Layer Theory. New York, NY: McGraw-Hill. Singleman, C. and Holtzman, N. G. (2014). Growth and Maturation in the Zebrafish, *Danio rerio*: A Staging Tool for Teaching and Research. *Zebrafish* 11, 396–406.

Singleman, C. and Holtzman, N. G. (2014). Growth and Maturation in the Zebrafish, Danio rerio: A staging tool for Teaching and Research. *Zebrafish* 11, 396-406

Stewart, W. J., Nair, A., Jiang, H. and McHenry, M. J. (2014). Prey fish escape by sensing the bow wave of a predator. *J. Exp. Biol* 217, 4328–4336.

Thielicke, W. and Stamhuis, E. J. (2014). PIVlab – Towards User-friendly, Affordable and Accurate Digital Particle Image Velocimetry in MATLAB. *J. Open Res. Softw.* 2, 1202–10.

van Netten, S. M. (2006). Hydrodynamic detection by cupulae in a lateral line canal: functional relations between physics and physiology. *Biol. Cybern.* 94, 67–85.

van Netten, S. M., Dinklo, T., Marcotti, W. and Kros, C. J. (2003). Channel gating forces govern accuracy of mechano-electrical transduction in hair cells. *Proc. Nat. Acad. Sci. USA* 100, 15510–15515.

van Netten, S. M. and Kroes, A. B. A. (1989). Dynamic Behavior and Micromechanical Properties of the Cupula. In The Mechanosensory Lateral Line (eds. S. Coombs, P. Go¨rner and H. Mu¨nz), pp. 247–263. New York, NY: Springer New York.

van Netten, S. M. and Kroese, A. B. A. (1987). Laser interferometric measurements on the dynamic behaviour of the cupula in the fish lateral line. *Hear. Res*. 29, 55–61.

van Netten, S. M. and McHenry, M. J. (2013). The Biophysics of Neuromasts. In Springer Handbook of Auditory Research 48: The Lateral Line. (eds. S. Coombs, H. Bleckmann, R. R. Fay and A. N. Popper), pp. 99–119. New York, NY: Springer New York.

Van Trump, W. J., Coombs, S., Duncan, K. and McHenry, M. J. (2010). Gentamicin is ototoxic to all hair cells in the fish lateral line system. *Hear. Res.* 261, 42–50.

Van Trump, W. J. and McHenry, M. J. (2008). The morphology and mechanical sensitivity of lateral line receptors in zebrafish larvae (*Danio rerio*). *J. Exp. Biol.* 211, 2105–2115.

Wada, H., Iwasaki, M. and Kawakami, K. (2014). Development of the lateral line canal system through a bone remodeling process in zebrafish. *Devel. Biol.* 392, 1–14.

Wark, A. R. and Peichel, C. L. (2010). Lateral line diversity among ecologically divergent threespine stickleback populations. *J. Exp. Biol.* 213, 108–17.

Webb, J. F. and Shirey, J. E. (2003). Postembryonic development of the cranial lateral line canals and neuromasts in zebrafish. *Devel. Dyn.* 228, 370–385.

Westphal, R. and O'Malley, D. (2013). Fusion of locomotor maneuvers, and improving sensory capabilities, give rise to the flexible homing strikes of juvenile zebrafish. *Front. Neur. Cir.* 7, 108.

Windsor, S. P. and McHenry, M. J. (2009). The influence of viscous hydrodynamics on the fish lateral-line system. *Integr. Comp. Biol.* 49, 691–701.

Wright, K. J., Higgs, D. M., Belanger, A. J., and Leis, J. M. (2005). Auditory and olfactory abilities of pre-settlement larvae and post-settlement juveniles of a coral reef damselfish (Pisces: Pomacentridae). *Mar. Biol.*, 147: 1425–1434

Yaniv S., Elad, D. and Holzman, R. (2014). Suction feeding across fish life stages: Flow dynamics from larvae to adults and implications for prey capture. *J. Exp. Biol.*, 217: 3748-3757

Yoshizawa, M., Jeffery, W. R., van Netten, S. M. and McHenry, M. J. (2014). The sensitivity of lateral line receptors and their role in the behavior of Mexican blind cavefish (*Astyanax mexicanus*). *J. Exp. Biol.* 217, 886–895.